grated reprogramming genes is often unmanageable, which might affect the differentiation potency of iPS cells and the safety of the iPS-derived cells. Thus, investigators have focused on generating iPS cells carrying no exogenous genetic materials either by repetitive transient gene expression (4, 5), by passive elimination of stable episomal DNA (6), or by recombinase-mediated excision of integrated genes from the chromosome (Refs. 7 and 8; for review, see Ref. 9). However, all of these approaches are not only inefficient but also laborious in practice, and development of a simpler gene delivery/expression system suitable for cell reprogramming is needed.

Sendai virus (SeV) is a nonsegmented negative-strand RNA virus belonging to the *Paramyxoviridae* (10). As SeV can infect various animal cells with an exceptionally broad host range and is not pathogenic to humans, various applications have been explored for SeV as a recombinant viral vector capable of transient but strong gene expression (11). We have demonstrated the potential of SeV as a tool for stable gene expression through an analysis of the Cl.151 strain (12). This unique variant was originally isolated as a mutant capable of persistent infection at a nonpermissive temperature (38 °C) (13). We cloned the entire genome of SeV Cl.151 and determined that more than two genetic elements were responsible independently for the establishment of stable persistent infections (12). We also demonstrated that SeV Cl.151 installed with a single exogenous gene could express it stably without chromosomal insertion (12). As this characteristic is advantageous for cell reprogramming, we planned to optimize this gene delivery/expression system through a more extensive analysis of SeV-mediated stable gene expression.

Here we describe the replication-defective and persistent Sendai virus (SeVdp) vector, a novel gene transfer/expression system based on SeV Cl.151, with the following characteristics, 1) efficient, harmless, and simultaneous delivery of up to four exogenous genes installed on a single vector, 2) stable and reproducible expression of installed genes at a pre-fixed balance without chromosomal integration, and 3) quick and complete erasure of the vector genome by interfering with viral RNA-dependent RNA polymerase using siRNA. We also demonstrated that an SeVdp vector installed with *Oct4*/*Sox2*/*Klf4*/*c-Myc* could reprogram mouse primary fibroblasts efficiently. These characteristics should make SeVdp a universal tool for stem cell research, especially for advanced cell reprogramming.

EXPERIMENTAL PROCEDURES

Reconstitution of SeVdp Vector by Reverse Genetics—All recombinant DNA experiments were performed according to our institutional guidelines and under the permission of the institutional recombinant DNA experiment committee of the National Institute of Advanced Industrial Science and Technology and of the National Institutes of Health Sciences. Replication-competent SeV was reconstituted as described (12). Full-length SeVdp vector genomic cDNA for SeV (Cl.151 strain and Nagoya strain) and for installed genes was constructed on the lambda Dash II vector as described in supplemental Fig. S1. In brief, the *M*, *F*, and *HN* genes were replaced with exogenous genes cloned between KasI and MluI restriction sites (for *M*), between BglII sites (for *F*), and between NheI and SphI sites (for *HN*). Additional extra genes were inserted into an NheI/NotI site created between the *P*/*C*/*V* and *M* genes. cDNAs encoding blasticidin S deaminase (*Bsr*), phleomycin-binding protein (*Zeo*), enhanced green fluorescent protein (*EGFP*), *Cypridina noctiluca* luciferase (*CLuc*), humanized Kusabira Orange (*KO*), and human gp91phox (*CYBB*) were amplified by polymerase chain reaction using pCX4-bsr (14), pUT58 (15), pEGFP-1 (Takara Bio, Otsu, Japan), pCLm (ATTO, Tokyo, Japan), phKO1-MN1 (Medical & Biological Laboratories, Nagoya, Japan), and gp91phox-pCI-neo as templates, respectively. cDNA encoding humanized Keima Red (*KR*) was synthesized by GenScript (Piscataway, NJ), according to a published peptide sequence (16).

The reconstructed cDNA plasmids (2 μg) and the expression vector plasmids for SeV nucleocapsid protein (NP), P/C, and L proteins (1 μg each) and pSRD-HN-Fmut (17) (2 μg) were transfected into BHK/T7/151M(SE) cells using Lipofectamine LTX Plus reagent (Invitrogen). BHK/T7/151M(SE) cells were established by expressing humanized T7 RNA polymerase and the M protein of the SeV Cl.151 strain stably in BHK-21 cells and cultured in Dulbecco's modified Eagle's medium (DMEM) supplemented with 10% fetal calf serum (FCS). The SeVdp vector was reconstituted in cells from positive-strand antigenome RNA transcribed from this cDNA and the SeV NP, P/C, L, Fmut, HN, and M (Cl.151) proteins. The vector-packaging cells harboring the SeVdp vector were established by selecting with antibiotics (blasticidin S at 10 μg/ml, zeocin at 500 μg/ml, or hygromycin B at 200 μg/ml) except for SeVdp(*c-Myc*/*Klf4*/*Oct4*/*Sox2*). The SeVdp vector was rescued by transient expression of the SeV *Fmut*, *HN*, and *M* (Cl.151) genes (driven by the SRα promoter derived from pcDL-SRα) (18) in the packaging cells as described above and recovered into the culture supernatant after incubation at 32 °C for 4 days. *Fmut*, a modified F gene for expressing the protease-susceptible SeV F protein, was generated as described (17). The supernatant was filtered through 0.45-μm cellulose acetate filters and stored in small aliquots at −80 °C. Titers of SeVdp vectors were determined by examining $LLCMK_2$ cells infected with a diluted SeVdp vector suspension using indirect immunofluorescence microscopy with an anti-NP rabbit polyclonal antibody.

Cell Culture, Fluorescence Microscopy, and Flow Cytometry—Long term stability of gene expression mediated by the SeVdp vectors was examined in $LLCMK_2$ cells and in human primary fibroblasts (TIG3) cultured in Eagle's minimum essential medium supplemented with 10% FCS. For examining stability under antibiotic selection, the cells were incubated in the presence of blasticidin S (Bs) (5 μg/ml), hygromycin B (200 μg/ml), or a mixture of blasticidin S (5 μg/ml) and zeocin (Zeo) (100 μg/ml). For examining stability without selection, the cells were preselected with antibiotics and then cultured without selection. The presence of SeVdp was determined by detecting SeV NP antigen with indirect immunofluorescence microscopy, counterstained with DAPI. EGFP, KO, and KR were detected by fluorescence microscopy (Zeiss, Oberkochen, Germany) using specific filters customized for these proteins. Flow cytometry was performed using a

FACSCalibur (BD Biosciences; see Figs. 2*B* and 3, *E* and *F*) and with FISHMAN R (On-chip Biotechnologies, Tokyo, Japan; Fig. 3, *G* and *H*) according to the standard procedures provided by the manufacturers.

Gene Delivery to Human Hematopoietic Stem Cells—All experiments using human resources were performed according to National Institute of Advanced Industrial Science and Technology and National Institutes of Health Sciences guidelines. OP9 cells (19) (provided by the RIKEN BioResource Center through the National Bio-Resource Project of the Ministry of Education, Culture, Sports, Science, and Technology of Japan) were cultured with minimal essential medium-α containing 20% FCS and 4 mM l-glutamine. Human umbilical cord blood was collected after a normal pregnancy and delivery after obtaining informed consent from the mothers. Human mononuclear cells were isolated from the cord blood using Lymphoprep (Axis-Shield, Oslo, Norway) according to the protocol provided by the manufacturer. CD133/1(+) cells were prepared from mononuclear cells using CD133 microbead kits and an AutoMACS system (Miltenyi Biotech, Bergisch Gladbach, Germany) with a purity greater than 90%, confirmed by flow cytometry using a FACSCalibur.

The purified CD133/1(+) cells were infected with SeVdp(*Bsr*/Δ*F*/*KO*) at a multiplicity of infection of 4 at 37 °C for 2 h. For examining the efficiency of gene delivery, the infected cells were cultured for 10 days in Iscove's modified Dulbecco's medium supplemented with 20% FCS, 8 mM L-glutamine, 50 μM 2-mercaptoethanol, 50 ng/ml human stem cell factor, 5 ng/ml interleukin-6 (IL-6), 5 ng/ml IL-3, 25 ng/ml flt-3 ligand (all from PeproTech, Rocky Hill, NJ), and 50 ng/ml human thrombopoietin (Kirin, Tokyo, Japan), and the fraction of KO-positive cells was determined by flow cytometry (Fig. 2*B*). For long term culture-initiating cell assays (20), 20- 200 SeVdp-infected cells were seeded on 1.25×10^4 γ-ray-irradiated OP9 cells in 96-well plates in Iscove's modified Dulbecco's medium with 12.5% FCS, 12.5% horse serum, 8 mM L-glutamine, 50 μM 2-mercaptoethanol, and 1 μM hydrocortisone for 5 weeks; half of the medium was exchanged every week. Then whole cells in a well were recovered and cultured in 300 μl of semisolid colony-forming cell assay medium (MethoCult GF+ H4433, StemCell Technologies, Vancouver, Canada) in 48-well plates. After culturing for 2 weeks, the numbers of KO-positive colonies were determined.

RNA Interference Analysis—The sequences of siRNAs against SeV *NP*, *P*, and *L* mRNAs (designed and synthesized by iGENE Therapeutics, Tokyo, Japan) used in this study are listed in supplemental Table S1. For examining the effect of siRNAs on the infection of replication-competent SeV vectors (supplemental Fig. S4*A*), 2×10^4 HeLa cells were seeded in 48-well plates with DMEM containing 10% FCS on day 0. On day 1, the cells were treated with siRNAs (100 nM) mixed with Lipofectamine 2000 (Invitrogen) for 6 h, then infected with SeV Cl.151(*EGFP*) at a multiplicity of infection of 100. The medium was replaced on day 2, and the cells were examined using fluorescence microscopy on day 4. For examining the effect of siRNAs on the removal of SeVdp vector from BHK-21 cells expressing the T7 RNA polymerase and F protein of the SeV Nagoya strain constitutively (BHK/T7/NaF cells) (supplemental Fig. S4*B*), 1×10^4 cells harboring SeVdp(*M*/*EGFP*/*Bsr*) were seeded in 48-well plates on day 0. On day 1 the cells were treated with siRNA (100 nM) mixed with Lipofectamine 2000 as described above. On day 5, the cells were examined using fluorescence microscopy. In both of these experiments, siRNA against firefly luciferase (21) was used as a control.

For examining the effect of siRNA on the removal of SeVdp vector using luciferase activity as a quantitative index (Fig. 4), 1.5×10^5 (Fig. 4*B*) or 3×10^4 (Fig. 4*C*) HeLa cells harboring SeVdp(*KO*/*Hyg*/*EGFP*/*Luc2CP*) were seeded with siRNAs (40 nM) mixed with Lipofectamine RNAiMAX (Invitrogen) as described above on day 0 in a 6-well plate (Fig. 4*B*) or in a 24-well plate (Fig. 4*C*), respectively. siRNA against *Renilla reniformis* luciferase (22) was used as a control. The cells were passaged with fresh siRNA on days 3 and 7, and the culture medium was replaced on the next day at each point. Firefly luciferase activity in the cell extract was determined on the indicated day using a luciferase assay system (Promega, Madison, WI). Specific luciferase activity was determined by normalizing against the amount of protein, determined using a Bradford protein assay kit (Bio-Rad). The cell lysates prepared on days 3, 7, and 12 were also analyzed by Western blotting using affinity-purified anti-SeV L protein rabbit antibody (2 μg/ml). For certifying complete removal of the SeVdp genome, the cells harboring SeVdp(*KO*/*Hyg*/*EGFP*/*Luc2CP*) and treated with siRNA as described above were cultured in the absence of siRNA for 4 weeks. Then, 1×10^4 of the cells were seeded in a 6-well plate and cultured in the presence of hygromycin B (100 μg/ml) for 10 days. The surviving cells were fixed, then stained with 0.01% crystal violet.

Biochemical Assays—SDS-PAGE and protein blotting were performed as described (23) using SuperSignal West Dura Extended Duration substrate (Thermo Fisher Scientific, Waltham, MA). For filter trap assays to detect the NP antigen (Table 1), culture supernatants of the cells harboring SeVdp vectors were passed through 0.45-μm cellulose acetate filters, trapped onto supported nitrocellulose membranes (0.2 μm, Bio-Rad) by vacuum filtration, and probed with an anti-SeV NP monoclonal mouse antibody.

Cell Reprogramming—Isolation and culture of mouse embryonic fibroblasts (MEFs) from a Nanog/GFP knock-in mouse (provided by the Riken BioResource Center) (MEF/Nanog-GFP), reprogramming with retroviral vectors and culture of mouse iPS cells were performed as described previously (24). Retroviral vectors installed separately with *Oct3/4*, *Sox2*, *Klf4*, and *c-Myc* (RvMX4) were prepared as described (1) using template DNA obtained from Addgene (Cambridge, MA). For reprogramming with SeVdp vectors installed with *Oct3/4*, *Sox2*, *Klf4*, and *c-Myc*, 1.25×10^5 of MEF/Nanog-GFP-expressing cells were infected with SeVdp vectors at 32 °C for 14 h. Then 1.0×10^3 of infected cells were seeded onto the feeder cells in 6-well plates and cultured as indicated in the legend to Fig. 5. The numbers of iPS colonies expressing GFP were determined using fluorescent microscopy. At 10 days after SeVdp infection, GFP-positive clones were isolated and treated with siRNA L527 as described above.

Characterization of iPS Cells—Semiquantitative RT-PCR Assays were performed using GoTaq qPCR Master Mix (Promega) and the primer sets listed in supplemental Table S2. Template cDNA was synthesized with random primers using SuperScript III reverse transcriptase (Invitrogen) from 2 μg of total cellular RNA isolated using ISOGEN (Nippon Gene, Tokyo, Japan). Bisulfite sequencing analysis was performed using the EpiTect Bisulfite kit (Qiagen, Hilden, Germany) with primer sets listed in supplemental Table S2. The PCR DNA fragments were cloned into pCR2.1 vector (Invitrogen), and sequenced by TAKARA BIO INC. (Shiga, Japan). Telomerase activity was determined using the Quantitative Telomerase Detection kit (Allied Biotech, Vallejo, CA). Teratoma formation was performed by subcutaneous injection of 1×10^6 SeVdp-iPS cells (clone #13) into SCID mice. Tumors recovered at necropsy after 6 weeks were processed for fixing and paraffin wax embedding, sectioned (4 μm), and stained with hematoxylin and eosin. Histological findings were evaluated using a DM3000 microscope (Leica, Wetzlar, Germany). Chimera animals were generated by microinjection of iPS cells into eight-cell or morula stage embryos. The embryos were collected in Medium 2 (Millipore, Billerica, MA) from oviduct and uterus of ICR female mice 2.5 days post-coitum. These embryos were transferred into potassium simplex optimized medium with amino acids (KSOM-AA, Millipore) and cultured for 1–2 h. iPS cells were trypsinized and suspended in iPS cell culture medium. A piezo-driven micro-manipulator (Prime Tech, Tokyo, Japan) was used to drill zona pellucida under the microscope, and 10–15 iPS cells were introduced into the subzonal space of individual 8-cell or morula-stage embryos. After injection, embryos underwent follow-up culture in KSOM-AA for 24 h (until blastomere stage) and then were transferred into the uteri of pseudopregnant recipient ICR female mice.

RESULTS

Basic Design of the SeVdp Vector—The SeV genome consists of six independent cistrons (NP, P/C/V, M, F, HN, and L), encoding eight proteins (10). Each cistron is preceded by a gene-start signal (3′-UCCCNNUUUC) and is followed by a gene-end signal (3′-AUUCUUUUU), which are the only essential *cis*-elements for transcription (25). This simple structure of each cistron makes it easier to design a defective viral vector by gene replacement. The *NP*, *P*, and *L* genes of SeV encode a major NP and two subunits of RNA-dependent RNA polymerase (P and L), respectively. All of these are indispensable for viral transcription and replication (10). We revealed previously that the *L* gene of the SeV Cl.151 strain with four missense mutations (V981I, S1088A, C1207S, and V1618L) contributes to long term persistence by providing the mechanism to escape from interferon β (IFNβ) induction (12). Among these mutations, V1618L is most critical; SeV with a mutant L protein (V1618L) is defective in IFNβ induction as with the Cl.151 strain.[4] We also found that uncapped read-through transcripts synthesized in an early stage of infection with wild-type SeV were only barely detectable in cells infected with SeV/L (V1618L).[4] We hypothesized that the defect in IFNβ induction might be correlated with the altered transcription of uncapped read-through RNA by the mutant SeV RNA polymerase.

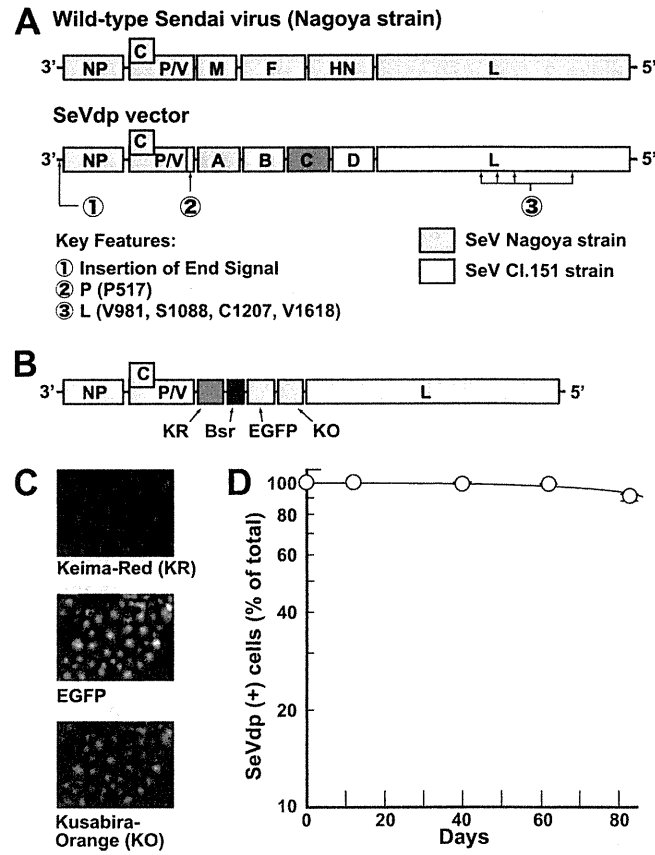

FIGURE 1. **Design and characteristics of the SeVdp vectors.** *A*, genome structure of the Sendai virus and an SeVdp vector is shown. Exogenous genes installed on the SeVdp vector are indicated as *A–D*. *B*, genome structure of SeVdp(*KR/Bsr/EGFP/KO*) is shown. *C*, expression of the fluorescent marker genes installed on the SeVdp vector is shown. $LLCMK_2$ cells were infected with SeVdp(*KR/Bsr/EGFP/KO*) at a multiplicity of infection of 0.1, selected with blasticidin S (5 μg/ml), and examined by fluorescence microscopy with dye-specific filters. *D*, stability of gene expression induced by the SeVdp vector is shown. $LLCMK_2$ cells were infected with SeVdp(*KR/Bsr/EGFP/KO*) and selected with blasticidin S as described in *C*. The cells were then cultured for the indicated period in the absence of blasticidin S. The ratio of SeV NP antigen-positive cells in the total cells was determined by fluorescence microscopy, as described under "Experimental Procedures."

In addition, we identified a missense mutation of the *P* gene (P517H) that is also essential for establishing long term persistency (Fig. 1*A*, supplemental Fig. S2*A*). The P protein makes a complex with the NP and L proteins, and the C terminus of P protein (amino acids, 479–568) has been assigned as a binding region for the NP (26). However, the precise role of this alteration in long term persistency remains to be determined. On the other hand, the 3′-distal region (nucleotides 1–2870) of the genome of SeV Cl.151 consists of the whole *NP* gene and part of the *P/C/V* genes but does not contribute to viral persistency (12) (Fig. 1*A*, supplemental Fig. S2*A*). Rather, we found that replacement of this 3′-distal region with that of the wild-type Nagoya strain significantly improved the recovery of the recombinant SeV from full-length genomic cDNA (supplemental Fig. S2*B*). We also inserted a

[4] K. Nishimura and M. Nakanishi, unpublished information.

gene-end signal just upstream of the gene-start signal of the *NP* gene (Fig. 1*A*, supplemental Fig. S2*C*). This modification further stabilized SeV-mediated gene expression through more stringent control of IFNβ induction by forced termination of uncapped read-through transcripts.[4]

We then planned to expand the capacity of the SeV Cl.151-based vector by deleting all the viral genes dispensable for stable gene expression. We have revealed previously that mutations within the central region (nucleotides 2871–9594) of the SeV Cl.151 genome contributed to viral persistence independently from the altered *L* gene (12). The region consists of *M*, *F*, and *HN* genes, which encode a matrix protein underlining the viral envelope (M) and envelope glycoproteins (F and HN), respectively. These structural genes are essential for production of infectious virions but are dispensable for viral transcription/replication, as SeV vectors with all of the *M*, *F*, and *HN* genes deleted could be generated successfully (27). However, as these defective vectors could not support stable gene expression, the role of these structural genes in long term persistency remains obscure.

We found previously that cells infected with SeV Cl.151 expressed large quantities of F and HN proteins on their surface (28). This observation suggested that the accumulation of the structural gene products (proteins and/or mRNAs) might interfere with the lytic infection cycle by a negative feedback mechanism, as proposed previously for the M protein (29). To examine this premise directly, we characterized recombinant SeVs with a dysfunction in each of the *M*, *F*, or *HN* genes either by deletion or by nonsense mutation. A selective marker gene (*Bsr*) conferring resistance to blasticidin S was used for estimating persistency rapidly (supplemental Fig. S3*A*). We found that all of these single-gene defective viruses established stable Bs-resistant colonies (supplemental Fig. S3*A*). Moreover, any two of these structural genes could be replaced with exogenous genes without affecting the persistent phenotype (supplemental Fig. S3*A*). To examine the role(s) of the M, F, and HN proteins further, we coexpressed these proteins directly from the cloned cDNAs and found that those derived from wild-type SeV strains induced much stronger cytopathic effects than did those derived from the SeV Cl.151 strain (supplemental Fig. S3*B*). From these results, we conclude that all of the *M*, *F*, and *HN* genes of SeV Cl.151 are dispensable and can be replaced with exogenous genes without disturbing viral persistency. We also succeeded in expanding the capacity of the vector by inserting an extra gene cassette between the *P*/*C*/*V* genes and the *M* gene without affecting viral persistency (Fig. 1*A*).

Dysfunction of structural genes is also essential for preventing self-replication of the vector. As the vectors used for cell reprogramming are installed with tumorigenic genes, such as *c-Myc* and *LIN28*, avoiding the production of secondary infectious particles from the gene-transferred cells is important not only to observe the regulation of recombinant DNA experiments but also to guarantee the safety of the vector in any therapeutic application. In the case of SeV, cultured cells infected with SeV variants defective in single structural genes produced significant amounts of virus-like particles (30, 31), suggesting that a dysfunction in single genes is insufficient for the complete blockage of self-replication. To reexamine this phenomenon, we determined the numbers of infectious particles and the amount of NP antigen in the culture supernatant of cells infected with various SeV Cl.151-derived defective viruses carrying the *Bsr* gene (Table 1). We found that cells infected with SeVs bearing a defect in one of the *F*, *HN*, or *M* genes produced significant amounts of NP antigen as well as infectious particles capable of transmitting Bs resistance to naïve cells (Table 1). This phenomenon was not observed when the viruses carried defects in at least two of the structural genes (Table 1). Therefore, we conclude that all three structural genes should be eliminated for maximizing the safety of the SeVdp vector through abolishing self-replication and for maximizing the vector capacity for installing exogenous genes.

TABLE 1

Determination of infectious virions and the NP protein in the culture supernatant of the cells harboring SeV Cl.151-based vectors

All the vectors were installed with the *Bsr* gene encoding blasticidine S deaminase. Aliquots of 10^6 of $LLCMK_2$ cells harboring each SeVdp vector were seeded in 90-mm wells with 8 ml of medium. After culturing for 3 days, culture supernatant was recovered and filtered through 0.45-μm cellulose acetate membranes. NP protein was determined by blotting 0.04–20 μl of the supernatant on nitrocellulose membranes as described under "Experimental Procedures." The supernatant was also incubated with 10^6 uninfected $LLCMK_2$ cells for 14 h and then cultured in the presence of Bs (10 μg/ml) for 7 days. The numbers of cell colonies resistant to Bs were determined by staining with crystal violet.

Structural genes			NP protein	Number of Bs^r colonies
			ng/day/10^5 cells	
M[a]	F[a]	HN[a]	8.75	$> 10^6$
–[b]	F	HN	5.36	366
M	–[b]	HN	7.62	2
M	F	–[b]	72.05	10
M	–[b]	–[b]	2.51[c]	0
–[b]	F	–[b]	2.76[c]	0
–[b]	–[b]	HN	2.61[c]	0
–[b]	–[b]	–[b]	2.56[c]	0

[a] Replication-competent vector.
[b] Corresponding genes were deleted or replaced with exogenous genes.
[c] Background caused by spontaneous cell lysis.

In summary, we have designed the basic genome structure of the SeVdp vector. This consists of three separate genetic elements (Fig. 1*A*) as follows. 1) The 3′-terminal structure comprises the *NP* and *P*/*C*/*V* genes derived from the Nagoya strain with an alteration for supporting stable gene expression. 2) Internal gene cassettes capable of installing up to four exogenous genes, created by deletion/replacement/insertion of *M*, *F*, and *HN* genes. 3) The *L* gene and the 5′-terminal structure derived from the Cl.151 strain with four missense mutations necessary for stable gene expression and for escaping from IFNβ induction.

Characterization of SeVdp Vector-mediated Gene Expression—We then prepared the SeVdp vectors installed with four exogenous genes and characterized vector-mediated gene expression. We first constructed SeVdp(*KR/Bsr/EGFP/KO*) installed with *Bsr* and three marker genes encoding KR, EGFP, and KO (Fig. 1*B*). All the cells infected with this vector expressed the three marker genes stably after selection with Bs (Fig. 1*C*). Furthermore, even in the absence of selection, 98.2% of cells retained the vectors for 62 days (Fig. 1*D*). Stability of gene expression induced by SeVdp vectors was solely dependent on the vector backbone described above and was not affected either by the installed genes or by the characteris-

TABLE 2

Stability of gene expression induced by SeVdp vectors

Cells harboring the SeVdp vectors were cultured in the presence of Bs (10 μg/ml) to certify that 100% of the cells were SeVdp (+). On day 0 the cells were set up in the medium either with Bs (Bs(+)) or without Bs (Bs(−)). Expression of SeV NP antigen was recorded periodically, and the day on which 100% ($T_{100\%}$), 95% ($T_{95\%}$), or 80% ($T_{80\%}$) of the cells expressed NP is indicated. The gene cassette no. corresponds to those shown in Fig. 1*A*. *Bsr*, blasticidin S deaminase; *KO*, Kusabira Orange; *EGFP*, enhanced green fluorescent protein; *CLuc*, *Cypridina noctiluca* luciferase; *CYBB*, gp91 phox; a*Gal*, human a-galactosidase; *KR*, Keima Red; ND, not determined because of the limited lifespan of the cells.

Gene cassette no.				Bs (−)		Bs (+)
A	B	C	D	$T_{95\%}$	$T_{80\%}$	$T_{100\%}$
					Days	
−[a]	*Bsr*	−[a]	*KO*	80[b]	205[b]	>180[b]
−[a]	*Bsr*	−[a]	*KO*	>80[c]	ND[c]	ND[c]
−[a]	*Bsr*	*EGFP*	*CLuc*	65[b]	105[b]	>180[b]
−[a]	*Bsr*	*EGFP*	*CYBB*	65[b]	170[b]	>180[b]
−[a]	*Bsr*	*EGFP*	*α-Gal*	60[b]	112[b]	>180[b]
KR	*Bsr*	*EGFP*	*KO*	70[b]	195[b]	>180[b]

[a] No exogenous gene was installed.
[b] Determined in $LLCMK_2$ cells.
[c] Determined in normal human fibroblasts.

tics of host cells (Table 2). Under selection with antibiotics, nearly 100% of cells could retain the expression of all the marker genes for at least 6 months (Table 2). Reflecting the characteristics of its parental virus, the SeVdp vector could deliver and express the installed genes stably in various host cells, including cell lines derived from the mouse (NIH3T3), hamster (CHO, BHK-21), monkey ($LLCMK_2$, CV-1, COS-7), and human (HeLa, U937) as well as human and mouse primary fibroblasts (12). Thus, we proved that the SeVdp vectors had preserved the same characteristics of the parental SeV Cl.151 to establish stable persistent infection after it had been modified with four exogenous genes.

We then examined the feasibility of using the SeVdp vectors in stem cell research, focusing on their biological inertness. Most gene delivery/expression systems using either recombinant viruses or physical/chemical means often trigger cellular defense systems against pathogenic microbes (32). The stimulated cells secrete various cytokines, which affect the proliferation, differentiation, and survival of stem cells. Wild-type SeV and conventional SeV vectors based on the wild-type Z strain powerfully induced the production of IFNβ, INFγ, TNFα, IL-1β, IL-6, IL-8, and many other cytokines (33–35), resulting in the apoptotic death of target cells. On the other hand, we revealed previously that SeV Cl.151 has a defect in inducing these inflammatory cytokines (12), suggesting strongly that the SeV Cl.151-based vector is biologically inert. To verify this under more stringent experimental conditions, we examined the effect of SeVdp-mediated gene transfer/expression on human hematopoietic stem cells (HSCs) by long term culture-initiating cell assays (20).

We isolated a CD133 (+) HSC-enriched fraction from human cord blood, infected it with the SeVdp vector bearing the *KO* gene (SeVdp(*Bsr*/ΔF/*KO*)) on day 0, and cultured it further in standard conditions. More than 90% of the cells in the HSC-enriched fraction were susceptible to the SeVdp vector under this infection protocol and sustained strong KO expression on days 3 (Fig. 2*A*) and 10 (Fig. 2*B*). Seven weeks after culturing on OP9 stromal cells, all kinds of myeloid lineage colonies derived from human HSCs, including colony-forming unit (CFU)-granulocytes (*CFU-G*), CFU-macrophages (*CFU-M*), CFU-granulocyte-macrophage , and burst-forming unit-erythroid (*BFU-E*) cells were readily detectable (Fig. 2*D–F*). Most importantly, 92% of these colonies still expressed KO very strongly on the seventh week (Fig. 2*C*), indicating that the SeVdp vector can deliver the gene quite efficiently into HSCs and is inert enough to sustain gene expression without affecting the differentiation of multipotent HSCs.

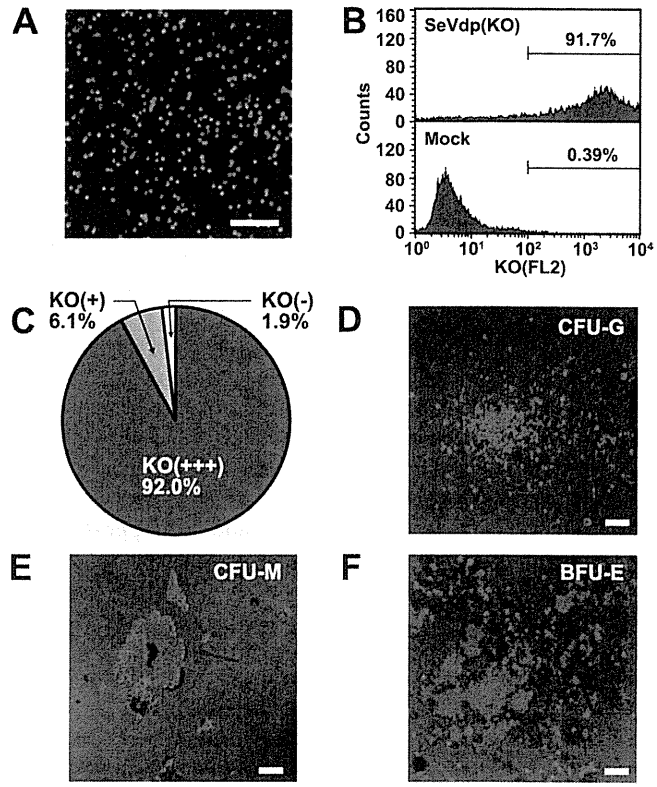

FIGURE 2. **Expression of KO in human hematopoietic stem cells and in their descendant cells.** *A* and *B*, expression of KO in CD133 (+) cord blood cells is shown. CD133 (+) cells were purified with magnetic beads conjugated with anti-CD133 antibody (Miltenyi Biotech). The cells were infected with SeVdp(*Bsr*/ΔF/*KO*) at a multiplicity of infection of 4 at 37 °C for 2 h. The cells were then cultured for 3 days (*A*) and 10 days (*B*) and examined using fluorescence and phase-contrast microscopy (*A*) and with flow cytometry using a FACSCalibur (BD Biosciences) (*B*), respectively. *C–F*, expression of KO in descendant colonies differentiated *in vitro* is shown. Cells infected with SeVdp(*Bsr*/ΔF/*KO*) as described above were cultured on OP9 cells in a 96-well plate for 5 weeks for lineage commitment. The cells in each well were then harvested, cultured in semisolid medium for 2 weeks, and examined for the expression of KO using fluorescence microscopy. *C*, the ratio of KO-positive colonies; 2931 differentiated colonies were examined. KO (+++), colonies expressing KO strongly; KO (+), colonies expressing KO weakly or heterogeneously; KO (−), colonies with no detectable KO expression. *D–F*, fluorescence and phase-contrast micrographs of typical colonies representative of each lineage. *D*, *CFU-G*, CFU-granulocytes. *E*, *CFU-M*, CFU-macrophages. *F*, *BFU-E*, burst-forming unit-erythroid cells. *Scale bar*, 100 μm.

For efficient and reproducible cell reprogramming, it is also important to express the various reprogramming genes at a fixed balance in each target cell (36–39). The SeVdp vector installed with four exogenous genes could deliver these genes simultaneously, so is theoretically superior to those systems delivering the genes separately. To clarify this issue further, we prepared an SeVdp vector installed with *KO* and *EGFP* together (SeVdp(*KO*/*Hyg*/*EGFP*/*Luc2CP*)) (Fig. 3*A*) and two

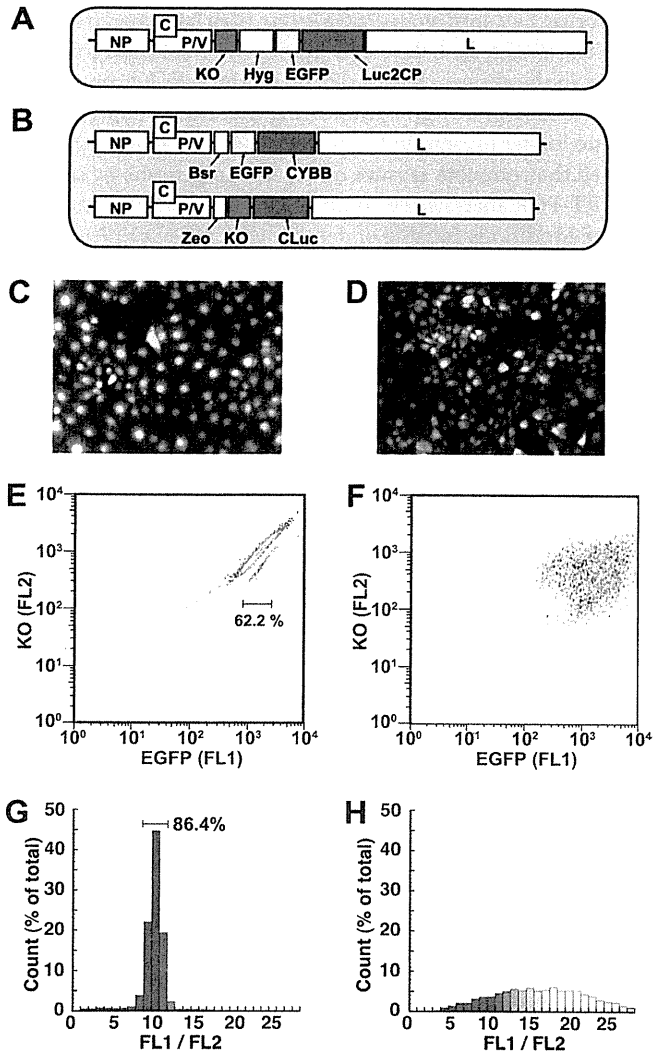

FIGURE 3. **Compatibility of two independent SeVdp vectors in a single cell.** *A*, genome structure of SeVdp(*KO/Hyg/EGFP/Luc2CP*) is shown. *B*, genome structure of SeVdp(*Bsr/EGFP/CYBB*) and SeVdp(*Zeo/KO/CLuc*), coexisting in a single cell is shown. *C* and *D*, fluorescence and phase-contrast micrographs of the cells described in schema (*C*) and in schema *B* (*D*) are shown. LLCMK$_2$ cells were infected with the SeVdp vectors as described in Fig. 1*C* and selected with hygromycin B (200 μg/ml) (*C*) or with zeocin (100 μg/ml) and blasticidin S (5 μg/ml) (*D*). Fluorescence images of KO and of EGFP were obtained separately with specific filter sets, converted to artificial color (*green* for EGFP and red for KO), and merged using iVision software (BioVision Technologies, Exton, PA). *E–H*, quantitative analysis of EGFP and KO expression by flow cytometry is shown. The cells shown in *C* (*E* and *G*) or in *D* (*F* and *H*) were harvested as single-cell suspensions with trypsin, and the fluorescent signals were analyzed using a FACSCalibur (BD Biosciences) for quantifying the signals of EGFP (FL1, 515–545 nm) and KO (FL2, 564–606 nm) after compensation (*E* and *F*) and analyzed with FISHMAN R (On-tip Biotechnologies) for determining the ratio of the signals of EGFP and KO in each cell as a histogram (*G* and *H*).

others installed with *KO* and *EGFP* separately on different SeVdp vectors (SeVdp(*Bsr/EGFP/CYBB*) and SeVdp(*Zeo/KO/CLuc*)) (Fig. 3*B*). We then characterized the expression levels of KO and EGFP induced by a single infection with SeVdp(*KO/Hyg/EGFP/Luc2CP*) and by coinfection with SeVdp(*Bsr/EGFP/CYBB*) and SeVdp(*Zeo/KO/CLuc*) (Fig. 3). When the cells were infected solely with SeVdp(*KO/Hyg/EGFP/Luc2CP*) (Fig. 3*A*), they expressed both KO (*red*) and EGFP (*green*) at a constant balance, shown by a uniform yellow color in merged microscopy images (Fig. 3*C*). In contrast, the cells coinfected with SeVdp(*Bsr/EGFP/CYBB*) and SeVdp(*Zeo/KO/CLuc*) (Fig. 3*B*) expressed KO and EGFP at a significantly different balance even after selection under Zeo plus Bs conditions (Fig. 3*D*). We then examined these cells quantitatively by flow cytometry (Fig. 3, *E–H*). When coinfected with SeVdp(*Bsr/EGFP/CYBB*) and SeVdp(*Zeo/KO/CLuc*), nearly 100% of the infected cells expressed both KO and EGFP after antibiotic selection (Fig. 3*F*), but the balance of expression varied widely (Fig. 3, *F* and *H*). In contrast, 86.4% of the cells infected with SeVdp(*KO/Hyg/EGFP/Luc2CP*) expressed KO and EGFP at a fixed balance (Fig. 3, *E* and *G*) and at a constant level (62.2% of the cells expressed EGFP and KO within a 3-fold range) (Fig. 3*E*). From these results, we conclude that only the SeVdp vector installed with all the genes required to be expressed from a single genome can express these genes reproducibly at a fixed balance, thus providing a significant advantage for cell reprogramming.

Elimination of SeVdp Vector with siRNA—The last hurdle for efficient cell reprogramming is to establish a method for eliminating the vector genome from those cells harboring it stably. Although the viral family *Paramyxoviridae* includes major human pathogens (*e.g.* measles virus and respiratory syncytial virus), there is no specific small-molecule antiviral drug available. Instead, siRNAs against viral genes have been investigated with the aim of interfering with viral replication (40). However, the effects of siRNAs on stable persistent infections such as the SeVdp system have not been established. Therefore, we examined the effect of knocking down the viral replication machinery on the stability of the SeVdp genome using specific siRNAs. We designed siRNAs against each of the *NP*, *P*, and *L* genes (Fig. 4*A*) and examined their effects on the infection of a replication-competent SeV Cl.151 installed with the *EGFP* gene (SeV Cl.151(*EGFP*)). When the cells were treated with these siRNAs just before infection, the replication of SeV Cl.151(*EGFP*) was blocked almost completely (supplemental Fig. S4*A*). However, the effects of these siRNAs on the cells already harboring an SeVdp vector stably were quite different; siRNA against the *L* gene was most effective, and that against the *NP* gene showed almost no effect (supplemental Fig. S4*B*). This phenomenon might simply reflect the relative abundance of the target gene products; *NP* mRNA is about 34 times more abundant than *L* mRNA (41). Otherwise, suppression of a catalytic subunit of RNA polymerase (L protein) might interfere with the replication of the SeVdp genome more profoundly.

We then examined the time course with which an SeVdp vector would be eliminated by siRNA against the *L* gene (Fig. 4). To monitor elimination quantitatively, we used a cell line harboring the SeVdp vector installed with a destabilized firefly luciferase gene (SeVdp(*KO/Hyg/EGFP/Luc2CP*)) and determined luciferase activity as a faithful marker of gene expression from the SeVdp vector. As shown in Fig. 4*B*, the siRNA blocked expression of the L protein quite efficiently after day 3. In parallel with this suppression, the SeVdp was eliminated at a half-life of 17.5 h after a short time lag: the luciferase activity fell below the detection limit after day 8 (Fig. 4*C*). This elimination was irreversible; when the cells

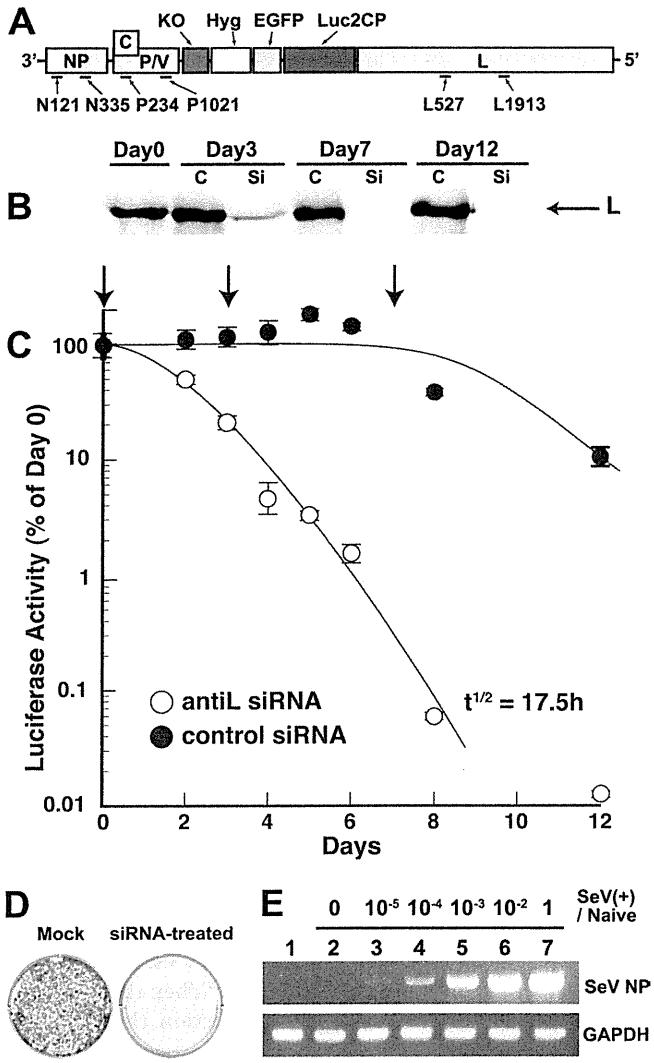

FIGURE 4. **Elimination of SeVdp vectors from the cells with specific siRNAs.** *A*, the genome structure of SeVdp(*KO/Hyg/EGFP/Luc2CP*) and target sites of siRNAs is shown. *B*, quantitative analysis of L protein by Western blotting is shown. HeLa cells carrying SeVdp(*KO/Hyg/EGFP/Luc2CP*) were cultured in the absence of hygromycin B and treated with siL527 (*Si*) or with control siRNA (*C*) complexed with Lipofectamine RNAiMAX (Invitrogen) on days 0, 3, and 7. The cells were harvested periodically as indicated, and 50-μg aliquots of cell extracts were separated on SDS-PAGE. The amount of L protein was determined by Western blotting probed with an anti-SeV L protein rabbit polyclonal antibody. *C*, quantitative analysis of SeVdp-mediated gene expression is shown. The HeLa cells carrying SeVdp(*KO/Hyg/EGFP/Luc2CP*) were treated with siRNA as described in *B*. The cells were harvested periodically as indicated, and the specific firefly luciferase activity was determined as described under "Experimental Procedures." *Open circles*, treated with siL527; *closed circles*, treated with control siRNA; *vertical arrows*, the day of siRNA treatment. *D*, detection of the cells carrying the SeVdp vector after treatment with siL527 is shown. HeLa cells carrying SeVdp(*KO/Hyg/EGFP/Luc2CP*) and treated with siL527 for 8 days as described in *C* were further cultured for 4 weeks in the absence of the siRNA and of hygromycin B. Aliquots of 1×10^4 cells were then seeded into 6-well plates with medium containing hygromycin B (100 μg/ml) and cultured for 10 days. The cells were fixed then stained with 0.01% crystal violet. *E*, detection of SeVdp by semiquantitative RT-PCR is shown. cDNAs were prepared by using 2-μg aliquots of total cellular RNAs as indicated, and the cDNA corresponding to 10^4 cells was analyzed by RT-PCR to determine SeV NP mRNA as described under "Experimental Procedures." *Lane 1*, HeLa cells carrying SeVdp(*KO/Hyg/EGFP/Luc2CP*) and treated with siL527 as described in *D*; *lanes 2–7*, naïve HeLa cells containing SeVdp(+) cells at the ratio indicated.

harboring SeVdp(*KO/Hyg/EGFP/Luc2CP*) had been treated with the siRNA for 8 days and were further cultured for 4 weeks in the absence of the siRNA, all the cells became susceptible to hygromycin B, indicating that the SeVdp genome was no longer present in the cells (Fig. 4*D*). We further confirmed the complete erasure of the SeVdp genome by sensitive RT-PCR analysis; we could not detect any SeV genome under conditions capable of detecting a single SeV(+) cell among 10^5 naïve cells (Fig. 4*E*). From these data, we conclude that siRNA against the L gene is an effective tool for erasing the SeVdp genome thoroughly from the cells.

Generation of Mouse iPS Cells with SeVdp Vectors Installed with Reprogramming Genes—We then constructed an SeVdp vector installed with four reprogramming genes (SeVdp(*c-Myc/Klf4/Oct4/Sox2*)) (Fig. 5*A*) and examined its potential to reprogram mouse fibroblasts. First, we compared the efficiency of reprogramming by an infection of SeVdp(*c-Myc/Klf4/Oct4/Sox2*) with that produced by the coinfection of ecotropic retrovirus vectors installed with the same genes separately (RvMX4), which is a current standard approach for iPS generation (24) (Fig. 5*C*). For assessing the expression of Nanog, a well known marker of fully reprogrammed iPS cells, we used embryonic fibroblasts derived from a Nanog-GFP knock-in mouse (MEF/Nanog-GFP) (24) and monitored the expression of GFP. We found that SeVdp(*c-Myc/Klf4/Oct4/Sox2*) and pMX4 reprogrammed 0.83 and 0.01% of MEF cells to Nanog (+) iPS cell-like colonies, respectively, on day 14 after vector infection (Fig. 5*C*). As the efficiency of emergence of Nanog-GFP (+) colonies from MEF with retrovirus vectors was consistent with that reported previously (24), we concluded that the SeVdp vector could reprogram MEF about 100 times more efficiently than standard procedures using retrovirus vectors. We also prepared SeVdp vectors installed with *Klf4/Oct4/Sox2* genes (SeVdp(*Klf4/Oct4/Sox2*)) and with a *c-Myc* gene (SeVdp(*Zeo/hKO/c-Myc*)) (Fig. 5*B*) separately. We found that the coinfection with these two SeVdp vectors reprogrammed MEF/Nanog-EGFP much less efficiently than did the single infection with SeVdp(*c-Myc/Klf4/Oct4/Sox2*) (Fig. 5*D*). These results clearly proved our assumption that installing all the necessary genes on a single vector was critical for maximizing the potential of the vector to reprogram cells.

After treating these Nanog (+) cells with siRNA L527, we obtained SeV antigen-free iPS cells with typical characteristics (Fig. 5). First, they expressed ES/iPS cell markers detectable by fluorescence microscopy (*Nanog*, *Sox2*, and *SSEA-1*) (Fig. 5*E*) as well as by RT-PCR (*Nanog*, *Sox2*, *Oct4*, *c-Myc*, *ECAT1*, and *FGF4*) (Fig. 5*F*). The primer sets used in this RT-PCR assay detected the expression of mouse genes but not that of human genes installed on the SeVdp vector. Some of the endogenous iPS marker genes (Nanog, Oct4, and Sox2) were detectable as early as on day 5 after gene transfer (Fig. 5*F*, *lane 3*), suggesting rapid cell reprogramming by the SeVdp vector. Second, the promoter regions of the *Oct4* and *Nanog* genes were epigenetically remodeled similar to ES cells (Fig. 5*G*). Third, telomerase activity was increased by 50–200-fold to the same level as in ES cells (Fig. 5*H*). Fourth, they differentiated into derivatives of all three germ layers in teratomas (Fig.

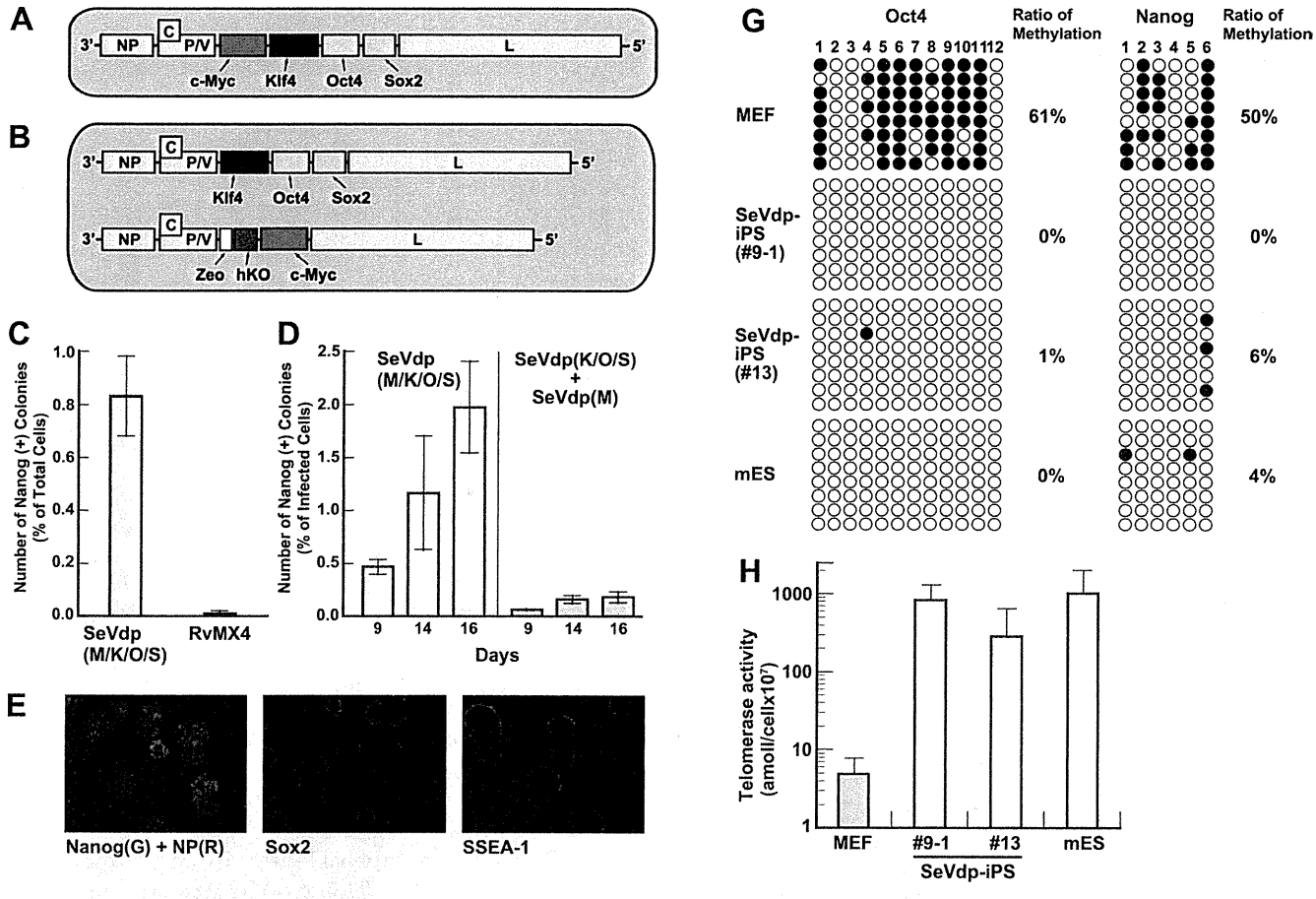

5*I*). Finally, we can generate chimera animals by injecting the SeVdp-iPS cells into embryos (Fig. 5*J*).

DISCUSSION

Discovery of the methods for achieving cell reprogramming with ectopic expression of defined factors has had a great impact on modern bioscience. However, to establish this technology for practical applications, we still have to overcome several difficult hurdles, such as the dramatic improvement of reprogramming efficiency and reproducible generation of fully differentiation-competent iPS cells without allowing the expression of residual exogenous genes on the chromosomes. Among these issues, chromosomal integration of reprogramming genes is the most critical factor affecting the characteristics of iPS cells (9). Incomplete suppression of exogenous reprogramming genes might affect the pluripotency of iPS cells. Furthermore, even if the integrated gene cassette is suppressed by epigenetic modification, differentiation of mouse iPS cells has frequently reactivated the integrated genes and induced cancers in iPS cell-derived offspring, as some of the reprogramming genes have intrinsic tumorigenic activity (24). Therefore, methodologies for generating fully pluripotent human iPS cells carrying no remnant of exogenous genes have been investigated but with limited success (9). As far as we know, the SeVdp vector described here is the only system that fulfills all the requirements to accomplish this goal with high efficiency and without laborious procedures.

Efficient gene delivery and expression are the primary factors affecting iPS cell generation, and this SeVdp vector has a great advantage over other delivery systems. As a typical recombinant viral vector, it can deliver genes much more efficiently than a nonviral system. In addition, its exceptionally broad host range should be quite beneficial; these viruses can infect almost all cell types from avian to human (42). Among others, the efficiency of the SeVdp vector to induce stable gene expression in human HSCs (~80%) is remarkably higher than that of retroviral vectors under multiple infection cycles with the aid of recombinant fibronectin fragments (~30%) (43). These characteristics have emerged partly because the SeVdp recognizes ubiquitous sialic acid as the primary receptor. Furthermore, the SeVdp has its own RNA-dependent RNA polymerase and requires only ubiquitous cytosolic proteins for transcription/replication (44). Thus, the SeVdp vector induces active transcription just after the nucleocapsid is delivered into the cytoplasm.

The enablement of stable gene expression without chromosomal integration is the most remarkable characteristic of these SeVdp vectors. DNA-based vectors (including retro/lentiviral vectors) can accomplish stable gene expression either by chromosomal integration or by episomal replication, depending on the cellular replication machinery. However, these characteristics make it difficult to remove the stabilized DNA from the cells; this depends either on a complex excision process using DNA recombinase or on passive elimination in the absence of selection. On the other hand, recombinant RNA viral vectors (except for retro/lentiviral vectors) cannot achieve stable gene expression, partly because they trigger cellular defense systems and induce apoptotic death in the host cells. The SeVdp vector is the only RNA-based platform inert enough to allow stable gene expression in sensitive HSCs, thanks to its unique gene mutations/alterations for escaping the host defense system. Furthermore, as the stability of SeVdp genomic RNA depends on the activity of viral RNA polymerase, interference of the polymerase with siRNA can be used to eliminate the genome from infected cells, as shown here.

Coinfection of conventional F-defective SeV vectors installed with *Oct4*, *Sox2*, *Klf4*, and *c-Myc* separately has been reported to generate iPS cells (45, 46). Although these reports demonstrated the potential of SeV vectors in cell reprogramming, our data have clearly demonstrated that this SeVdp vector provides a superior alternative to this approach. Among other factors, the cytopathic nature of the conventional SeV vectors based on wild-type SeV, including simple F-defective SeV vectors (30, 47), limits their utility in cell re-

FIGURE 5. **Reprogramming of MEFs with SeVdp vectors installed with reprogramming genes.** *A*, the genome structure of SeVdp(*c-Myc/Klf4/Oct4/Sox2*) is shown. *B*, shown is genome structure of SeVdp(*Klf4/Oct4/Sox2*) and SeVdp(*Zeo/hKO/c-Myc*), coexisting in a single cell, is shown. *C* and *D*, shown is the efficiency to reprogram MEF/Nanog-GFP. MEF/Nanog-GFP cells (1.25×10^5) were infected with SeVdp vectors, and retroviral vectors were installed with *c-Myc/Klf4/Oct4/Sox2* as described under "Experimental Procedures." Then 1.0×10^3 of infected cells were seeded onto the feeder cells in 6-well plates and cultured for 14 days (*C*) or for the indicated days (*D*). The number of iPS colonies expressing GFP was determined under fluorescent microscopy. Reprogramming efficiency was indicated as the ratio of the number of EGFP-positive colonies to that of MEF/Nanog-GFP seeded in the well (*C*) or to that of infected MEF/Nanog-GFP seeded in the well (*D*). *C*, shown is a comparison of reprogramming efficiency with the SeVdp(*c-Myc/Klf4/Oct4/Sox2*) vector and with retroviral vectors. *SeVdp(M/K/O/S)*, SeVdp(*c-Myc/Klf4/Oct4/Sox2*); *RvMX4*, coinfection of ecotropic retroviral vectors installed with *c-Myc*, *Klf4*, *Oct4*, and *Sox2* separately. *D*, shown is a comparison of reprogramming efficiency by a single infection of SeVdp(*c-Myc/Klf4/Oct4/Sox2*) (*SeVdp(M/K/O/S)*) and by coinfections of SeVdp(*Klf4/Oct4/Sox2*) and SeVdp(*Zeo/hKO/c-Myc*) (*SeVdp(K/O/S)* + *SeVdp(M)*). *E*, characterization of mouse iPS cells generated with SeVdp(*c-Myc/Klf4/Oct4/Sox2*) is shown. The ES-like colonies emerging from MEF/Nanog-GFP cell lines were fixed, incubated with specific primary antibodies against SeV NP antigen (*left*), Sox2 (*middle*), and SSEA-1 (*right*), then stained with secondary antibodies conjugated with Alexa 555. The cells were then counterstained with DAPI and examined by fluorescence microscopy as described under "Experimental Procedures." *Nanog* (*left*), expression of GFP driven by the Nanog promoter. *F*, gene expression analysis with semiquantitative RT-PCR is shown. Aliquots (2 μg) of total RNA prepared from the cells indicated were analyzed as described under "Experimental Procedures." *Lane 1*, MEF; *lane 2*, MEF infected with control vector (SeVdp(*Bsr/ΔF/KO*)); *lane 3*, MEF infected with SeVdp(*M/K/O/S*) on day 5 infection; *lane 4*, SeVdp-iPS cell clone #2-1; *lane 5*, SeVdp-iPS cell clone #9-1; *lane 6*, SeVdp-iPS cell clone #13; *lane 7*, SeVdp-iPS cell clone #16; *lane 8*, SeVdp-iPS cell clone #21; *lane 9*, mouse iPS cell generated with retrovirus vectors (RvMX4); *lane 10*, mouse ES cell (clone D3). *ECAT1*, ES cell-associated transcript 1; *FGF4*, fibroblast growth factor 4. *G*, methylation analysis of Oct4 and Nanog promoters is shown. Methylation profile of CpG in genomic DNA was analyzed by bisulfite sequence analysis as described under "Experimental Procedures." *Open circles*, unmethylated cytosine; *closed circles*, methylated cytosine. The ratio of methylated cytosine is indicated as a percentage of total cytosine residues analyzed. *H*, a telomerase assay is shown. Telomerase activity in total cell extract prepared from 1×10^3 cells was analyzed as described under "Experimental Procedures" and is indicated as the amount of $(dTTAGGG)_n$ synthesized. *I*, histology of teratomas derived from SeVdp-iPS cells is shown. Teratoma formation was studied at 6 weeks after the subcutaneous injection of 1×10^6 SeVdp-iPS cells from clone #13 into SCID mice. *a–c*, low magnification; *scale bar* = 100 μm. *d–h*, high magnification observation; *scale bar* = 20 μm. *d*, cartilage; *e*, epidermis; *f*, hair follicle; *g*, sweat gland; *h*, intestinal gland. *J*, adult chimeras derived from SeVdp-iPS cells (clone #13) are shown. *Dark hair* indicates donor contribution.

programming. As revealed in our previous work (12) and in the present article, the cytopathogenicity of SeV depends on multiple factors including escaping from cytokine induction and acute membrane dysfunction, and it is not possible to evade this by simple deletion of all the structural genes (*M*, *F*, and *HN*) (27). Furthermore, the use of a single-gene defective SeV vector raises safety and regulatory concerns, as the potential of the SeV vector to self-replicate was diminished but was not completely abolished by a single gene defect, as shown in Table 1. This issue was neither investigated nor addressed in previous reports describing single gene defective vectors (30, 47) but has been resolved here for the first time.

Cell reprogramming depends on the simultaneous delivery of multiple genes, on their balanced expression, and on their prompt suppression/removal. These factors affect both the efficiency of iPS cell generation and the quality of the iPS cells (36, 39). Nevertheless, this issue has not been investigated in detail, partly because most of the current viral vectors can accommodate only one or a few extra genes. The capacity of SeVdp vectors to install four reprogramming genes on a single vector was critical both for expressing these genes at a prefixed balance (Fig. 3) and for highly efficient reprogramming (Fig. 5); coinfection of two independent SeVdp vectors failed to accomplish either of these goals (Figs. 3 and 5). This latter phenomenon might be caused by homologous viral interference, which has been observed after coinfections of two independent paramyxoviruses including SeV (48). Otherwise, this phenomenon could reflect that the SeVdp genome is a multicopy replicon with about 40,000 copies per cell (12). In general, it is difficult to manage to produce two (or more) independent multicopy replicons under equal balance when they share the same replication machinery. Active and rapid erasure of SeVdp vectors with specific siRNAs (Fig. 4) is also advantageous to the generation of homogeneous and vector-free iPS cells compared with the passive and unmanageable vector removal that depends on the sequential passages of the cells (45, 46).

Synthetic modified mRNA encoding reprogramming factors has been reported to generate iPS cells highly efficiently (49). This nonviral approach and our SeVdp vector have their own advantages and disadvantages, but the escape from the cellular antiviral defense system is a critical characteristic common to these advanced reprogramming systems. The former has the advantage that the combination of exogenous reprogramming genes and the balance or duration of their expression can be adjusted flexibly. The nonviral approach has another advantage, as the use of recombinant viruses is regulated strictly in general. On the other hand, it is highly dependent on the gene delivery system, as it requires repetitive transfection for 16 days. Therefore, it might not be applicable to cells that are difficult to transfect, such as primary peripheral blood cells. In contrast, adjustment of reprogramming genes and of their expression is not so easy using SeVdp vectors and needs the construction of different vectors for tuning these features. However, once established, the SeVdp vector can always induce steady expression of the installed genes at a fixed balance, and this feature allows highly reproducible and uniform cell reprogramming. Furthermore, prolonged gene expression by a single infection procedure and the wider host range available are advantageous for practical applications, such as reprogramming of blood cells. Combining the results obtained with these two approaches depending on specific research purposes will enable us to create a more advanced system for cell reprogramming.

The field of cell reprogramming is expanding very rapidly, and the tools for safer and efficient reprogramming have become increasingly important both for basic research and for development of medical applications. We are presently investigating the utility of the SeVdp vectors in the genomic reprogramming of human cells.

Acknowledgments—We thank Dr. Hideharu Taira and Dr. Yutaka Takebe for providing pSRD-HN-Fmut and pcDL-SRα, respectively, and Dr. Akinori Masago for preparing anti-SeV L antibody and Naeko Sakai for excellent technical assistance.

REFERENCES

1. Takahashi, K., and Yamanaka, S. (2006) *Cell* **126,** 663–676
2. Müller, L. U., Daley, G. Q., and Williams, D. A. (2009) *Mol. Ther.* **17,** 947–953
3. Jaenisch, R., and Young, R. (2008) *Cell* **132,** 567–582
4. Okita, K., Nakagawa, M., Hyenjong, H., Ichisaka, T., and Yamanaka, S. (2008) *Science* **322,** 949–953
5. Jia, F., Wilson, K. D., Sun, N., Gupta, D. M., Huang, M., Li, Z., Panetta, N. J., Chen, Z. Y., Robbins, R. C., Kay, M. A., Longaker, M. T., and Wu, J. C. (2010) *Nat. Methods* **7,** 197–199
6. Yu, J., Hu, K., Smuga-Otto, K., Tian, S., Stewart, R., Slukvin, I. I., and Thomson, J. A. (2009) *Science* **324,** 797–801
7. Kaji, K., Norrby, K., Paca, A., Mileikovsky, M., Mohseni, P., and Woltjen, K. (2009) *Nature* **458,** 771–775
8. Woltjen, K., Michael, I. P., Mohseni, P., Desai, R., Mileikovsky, M., Hämäläinen, R., Cowling, R., Wang, W., Liu, P., Gertsenstein, M., Kaji, K., Sung, H. K., and Nagy, A. (2009) *Nature* **458,** 766–770
9. O'Malley, J., Woltjen, K., and Kaji, K. (2009) *Curr. Opin. Biotechnol.* **20,** 516–521
10. Lamb, R. A., and Kolakofsky, D. (2001) in *Fundamental Virology* (Knipe, D. M., and Howley, P. M., eds.) 4th Ed., pp. 689–724, Lippincott Williams & Wilkins, Philadelphia
11. Griesenbach, U., Inoue, M., Hasegawa, M., and Alton, E. W. (2005) *Curr. Opin. Mol. Ther.* **7,** 346–352
12. Nishimura, K., Segawa, H., Goto, T., Morishita, M., Masago, A., Takahashi, H., Ohmiya, Y., Sakaguchi, T., Asada, M., Imamura, T., Shimotono, K., Takayama, K., Yoshida, T., and Nakanishi, M. (2007) *J. Biol. Chem.* **282,** 27383–27391
13. Yoshida, T., Nagai, Y., Maeno, K., Iinuma, M., Hamaguchi, M., Matsumoto, T., Nagayoshi, S., and Hoshino, M. (1979) *Virology* **92,** 139–154
14. Akagi, T., Sasai, K., and Hanafusa, H. (2003) *Proc. Natl. Acad. Sci. U.S.A.* **100,** 13567–13572
15. Drocourt, D., Calmels, T., Reynes, J. P., Baron, M., and Tiraby, G. (1990) *Nucleic. Acids Res.* **18,** 4009
16. Kogure, T., Karasawa, S., Araki, T., Saito, K., Kinjo, M., and Miyawaki, A. (2006) *Nat. Biotechnol.* **24,** 577–581
17. Taira, H., Sato, T., Segawa, H., Chiba, M., Katsumata, T., and Iwasaki, K. (1995) *Arch. Virol.* **140,** 187–194
18. Takebe, Y., Seiki, M., Fujisawa, J., Hoy, P., Yokota, K., Arai, K., Yoshida, M., and Arai, N. (1988) *Mol. Cell. Biol.* **8,** 466–472
19. Nakano, T., Kodama, H., and Honjo, T. (1994) *Science* **265,** 1098–1101
20. Croisille, L., Auffray, I., Katz, A., Izac, B., Vainchenker, W., and Coulombel, L. (1994) *Blood* **84,** 4116–4124
21. Elbashir, S. M., Harborth, J., Lendeckel, W., Yalcin, A., Weber, K., and Tuschl, T. (2001) *Nature* **411,** 494–498
22. Sano, M., Sierant, M., Miyagishi, M., Nakanishi, M., Takagi, Y., and

Sutou, S. (2008) *Nucleic. Acids Res.* **36,** 5812–5821
23. Okabe, J., Eguchi, A., Wadhwa, R., Rakwal, R., Tsukinoki, R., Hayakawa, T., and Nakanishi, M. (2004) *Hum. Mol. Genet.* **13,** 285–293
24. Okita, K., Ichisaka, T., and Yamanaka, S. (2007) *Nature* **448,** 313–317
25. Plattet, P., Strahle, L., le Mercier, P., Hausmann, S., Garcin, D., and Kolakofsky, D. (2007) *Virology* **362,** 411–420
26. Horikami, S. M., Smallwood, S., and Moyer, S. A. (1996) *Virology* **222,** 383–390
27. Yoshizaki, M., Hironaka, T., Iwasaki, H., Ban, H., Tokusumi, Y., Iida, A., Nagai, Y., Hasegawa, M., and Inoue, M. (2006) *J. Gene Med.* **8,** 1151–1159
28. Eguchi, A., Kondoh, T., Kosaka, H., Suzuki, T., Momota, H., Masago, A., Yoshida, T., Taira, H., Ishii-Watabe, A., Okabe, J., Hu, J., Miura, N., Ueda, S., Suzuki, Y., Taki, T., Hayakawa, T., and Nakanishi, M. (2000) *J. Biol. Chem.* **275,** 17549–17555
29. Ogino, T., Iwama, M., Ohsawa, Y., and Mizumoto, K. (2003) *Biochem. Biophys. Res. Commun.* **311,** 283–293
30. Inoue, M., Tokusumi, Y., Ban, H., Kanaya, T., Tokusumi, T., Nagai, Y., Iida, A., and Hasegawa, M. (2003) *J. Virol.* **77,** 3238–3246
31. Sugahara, F., Uchiyama, T., Watanabe, H., Shimazu, Y., Kuwayama, M., Fujii, Y., Kiyotani, K., Adachi, A., Kohno, N., Yoshida, T., and Sakaguchi, T. (2004) *Virology* **325,** 1–10
32. Takeuchi, O., and Akira, S. (2010) *Cell* **140,** 805–820
33. Hua, J., Liao, M. J., and Rashidbaigi, A. (1996) *J. Leukoc. Biol.* **60,** 125–128
34. Murakami, Y., Ikeda, Y., Yonemitsu, Y., Tanaka, S., Kondo, H., Okano, S., Kohno, R., Miyazaki, M., Inoue, M., Hasegawa, M., Ishibashi, T., and Sueishi, K. (2008) *J. Gene Med.* **10,** 165–176
35. Zidovec, S., and Mazuran, R. (1999) *Cytokine* **11,** 140–143
36. Papapetrou, E. P., Tomishima, M. J., Chambers, S. M., Mica, Y., Reed, E., Menon, J., Tabar, V., Mo, Q., Studer, L., and Sadelain, M. (2009) *Proc. Natl. Acad. Sci. U.S.A.* **106,** 12759–12764
37. Carey, B. W., Markoulaki, S., Hanna, J., Saha, K., Gao, Q., Mitalipova, M., and Jaenisch, R. (2009) *Proc. Natl. Acad. Sci. U.S.A.* **106,** 157–162
38. Gonzalez, F., Barragan Monasterio, M., Tiscornia, G., Montserrat Pulido, N., Vassena, R., Batlle Morera, L., Rodriguez Piza, I., and Izpisua Belmonte, J. C. (2009) *Proc. Natl. Acad. Sci. U.S.A.* **106,** 8918–8922
39. Chin, M. H., Pellegrini, M., Plath, K., and Lowry, W. E. (2010) *Cell Stem Cell* **7,** 263–269
40. Haasnoot, J., Westerhout, E. M., and Berkhout, B. (2007) *Nat. Biotechnol.* **25,** 1435–1443
41. Homann, H. E., Hofschneider, P. H., and Neubert, W. J. (1990) *Virology* **177,** 131–140
42. Nakanishi, M., Mizuguchi, H., Ashihara, K., Senda, T., Akuta, T., Okabe, J., Nagoshi, E., Masago, A., Eguchi, A., Suzuki, Y., Inokuchi, H., Watabe, A., Ueda, S., Hayakawa, T., and Mayumi, T. (1998) *J. Control Release* **54,** 61–68
43. Hanenberg, H., Hashino, K., Konishi, H., Hock, R. A., Kato, I., and Williams, D. A. (1997) *Hum. Gene Ther.* **8,** 2193–2206
44. Ogino, T., Kobayashi, M., Iwama, M., and Mizumoto, K. (2005) *J. Biol. Chem.* **280,** 4429–4435
45. Fusaki, N., Ban, H., Nishiyama, A., Saeki, K., and Hasegawa, M. (2009) *Proc. Jpn. Acad. Ser. B Phys. Biol. Sci.* **85,** 348–362
46. Seki, T., Yuasa, S., Oda, M., Egashira, T., Yae, K., Kusumoto, D., Nakata, H., Tohyama, S., Hashimoto, H., Kodaira, M., Okada, Y., Seimiya, H., Fusaki, N., Hasegawa, M., and Fukuda, K. (2010) *Cell Stem Cell* **7,** 11–14
47. Li, H. O., Zhu, Y. F., Asakawa, M., Kuma, H., Hirata, T., Ueda, Y., Lee, Y. S., Fukumura, M., Iida, A., Kato, A., Nagai, Y., and Hasegawa, M. (2000) *J. Virol.* **74,** 6564–6569
48. Shimazu, Y., Takao, S. I., Irie, T., Kiyotani, K., Yoshida, T., and Sakaguchi, T. (2008) *Virology* **372,** 64–71
49. Warren, L., Manos, P. D., Ahfeldt, T., Loh, Y. H., Li, H., Lau, F., Ebina, W., Mandal, P. K., Smith, Z. D., Meissner, A., Daley, G. Q., Brack, A. S., Collins, J. J., Cowan, C., Schlaeger, T. M., and Rossi, D. J. (2010) *Cell Stem Cell* **7,** 618–630

ELSEVIER

Experimental Hematology

Experimental Hematology 2012;40:166–174

Homeostasis of hematopoietic stem cells regulated by the myeloproliferative disease associated-gene product Lnk/Sh2b3 via Bcl-xL

Nao Suzuki[a,b], Satoshi Yamazaki[c], Hideo Ema[a], Tomoyuki Yamaguchi[a,c], Hiromitsu Nakauchi[a,c], and Satoshi Takaki[b]

[a]*Laboratory of Stem Cell Therapy, Center for Experimental Medicine, The Institute of Medical Science, University of Tokyo, Tokyo, Japan;* [b]*Department of Immune Regulation, Research Institute, National Center for Global Health and Medicine, Tokyo, Japan;* [c]*Japan Science Technology Agency, Exploratory Research for Advanced Technology (ERATO) Nakauchi Stem Cell and Organ Regeneration Project, Tokyo, Japan*

(Received 31 August 2011; revised 25 October 2011; accepted 9 November 2011)

Hematopoietic stem cells (HSCs) are maintained at a very low frequency in adult bone marrow under steady-state conditions. However, it is not fully understood how homeostasis of bone marrow HSCs is maintained. We attempted to identify a key molecule involved in the regulation of HSC numbers, a factor that, in the absence of *Lnk*, leads to HSC expansion. Here, we demonstrate that upon stimulation with thrombopoietin, expression of Bcl-xL, an antiapoptotic protein, was highly enhanced in *Lnk*-deficient HSCs compared to normal HSCs. As a result, *Lnk*-deficient HSCs underwent reduced apoptosis following exposure to lethal radiation. Downregulation of *Bcl-xL* expression in *Lnk*-deficient HSCs by short-hairpin RNA resulted in a great reduction of their capacity for reconstitution. These findings suggest that Lnk/Sh2b3 constrains the expression of Bcl-xL and that the loss of Lnk/Sh2b3 function enhances survival of HSCs by inhibiting apoptosis. Furthermore, our observations indicate that HSCs in patients with an Lnk/Sh2b3 mutation might become resistant to apoptosis due to thrombopoietin-mediated enhanced expression of Bcl-xL. Consequently, reduced apoptosis could facilitate accumulation of HSCs with oncogenic mutations leading to development of myeloproliferative disorders. © **2012 ISEH - Society for Hematology and Stem Cells. Published by Elsevier Inc.**

Hematopoietic stem cells (HSCs) have both self-renewal and multilineage differentiation potential. They are among the most important somatic stem cells and sustain life by supplying all mature blood and immune cells. HSCs are maintained at a very low frequency and the majority are maintained in quiescence in adult bone marrow (BM) during steady-state demand. Although the mechanisms maintaining a small pool of HSCs are not fully understood, previous reports showed that homeostasis of HSCs is influenced by the BM microenvironment, called the "HSC niche," in which HSCs reside and self-renew. Depletion or reduction of cells constituting the HSC niche decreases the number of HSCs, although the identity of the HSC niche is still uncertain [1–4]. On the other hand, it has been shown that HSC pools can be greatly expanded independent of the HSC niche by forced expression of transcription factor *HoxB4* [5,6] or the lack of intracellular adaptor protein Lnk/Sh2b3 in HSCs [7].

Lnk/Sh2b3 is an intracellular signal transduction protein containing a proline-rich domain, a pleckstrin homology domain, and an Src homology 2 domain [8]. In $Lnk^{-/-}$ mice, long-term BM repopulating activity is markedly elevated because of increases in both the absolute number and self-renewal capacity of HSCs [7,9]. Recent reports indicated that Lnk/Sh2b3 directly inhibits the Janus activating kinase (JAK) 2–signal transducers and activators of transcription (STAT) 5 pathway activated through thrombopoietin (TPO)-c-Mpl signaling in HSCs and megakaryocytes [10–12]. In addition to STAT5, Akt was further activated in $Lnk^{-/-}$ HSCs via TPO-c-Mpl signaling. However, the molecular mechanism for HSC expansion downstream from those signaling pathways remains

Offprint requests to: Hiromitsu Nakauchi, M.D., Ph.D., Laboratory of Stem Cell Therapy, Center for Experimental Medicine, The Institute of Medical Science, University of Tokyo, 4-6-1 Shirokanedai, Minato-ku, Tokyo 108-8639, Japan; E-mail: nakauchi@ims.u-tokyo.ac.jp and Satoshi Takaki, M.D., Ph.D., Department of Immune Regulation, Research Institute, National Center for Global Health and Medicine, 1-21-1 Toyama, Shinjuku-ku, Tokyo 162-8655, Japan; E-mail: stakaki@ri.ncgm.go.jp

Supplementary data related to this article can be found online at doi:10.1016/j.exphem.2011.11.003.

doi: 10.1016/j.exphem.2011.11.003

unclear. To identify key molecule(s) intrinsically expressed in HSC and involved in the regulation of homeostasis in HSCs, we focused on members of the antiapoptotic Bcl-2 gene family, *Bcl-xL* and *Bcl-2*. These genes are transcriptionally regulated by phospho-STAT5 when the JAK-STAT pathway is activated through the erythropoietin receptor or other cytokine signaling [13,14]. $STAT5^{-/-}$ embryos show severe anemia due to facilitated apoptosis of erythroid progenitors by reduced expression of Bcl-xL [13]. Here we reveal that Bcl-xL, but not Bcl-2, is highly accumulated in HSCs and progenitors upon stimulation with TPO in the absence of Lnk/Sh2b3. As a result, $Lnk^{-/-}$ HSCs were resistant to DNA damage induced by irradiation. Short-hairpin RNA (shRNA)-mediated downregulation of *Bcl-xL* expression in *Lnk*-deficient HSCs resulted in a significant reduction of reconstitutional capacity comparable to that of normal HSCs. Our results indicated that Lnk/Sh2b3 constrains expression of Bcl-xL and participates in the regulation of HSC homeostasis by maintaining proper responses against various proapoptotic stimuli.

Materials and methods

Mice

C57BL/6 mice congenic for the Ly5 locus (B6-Ly5.1) and $Lnk^{-/-}$ B6-Ly5.1 mice were bred and maintained at the Animal Research Center of the Institute of Medical Science, University of Tokyo. The Animal Experiment Committee of the Institute of Medical Science, University of Tokyo, approved animal care and use. B6-Ly5.1/5.2 (B6-F1) mice were obtained from mating pairs of B6-Ly5.1 and B6-Ly5.2 mice. B6-Ly5.2 mice were purchased from Nihon SLC (Shizuoka, Japan).

Purification of $CD34^{-}$KSL cells

$CD34^{-}$KSL cells were purified from BM cells of 7- to 10-week-old wild-type (WT) or $Lnk^{-/-}$ B6 Ly5.1 mice as described [15,16]. In brief, whole BM cells were stained with an antibody mixture consisting of biotinylated anti–Gr-1, Mac-1, B220, CD4, CD8, interleukin-7Ra, and Ter-119 monoclonal antibodies (Pharmingen, San Diego, CA, USA). Lineage-positive cells were depleted with streptavidin magnetic beads and MACS LS column (Miltenyi Biotech, Bergish Gladbach, Germany). Cells were further stained with fluorescein isothiocyanate–conjugated anti-CD34, phycoerythrin (PE)-conjugated anti–Sca-1, and allophycocyanin-conjugated anti–c-Kit antibodies (Pharmingen). Biotinylated antibodies were detected with streptavidin-allophycocyanin-Cy7 (eBioscience, San Diego, CA, USA). Four-color immunostaining analysis and sorting were performed on a FACSAria (Becton Dickinson, San Jose, CA, USA).

Intracellular staining

Freshly isolated BM cells or cells cultured for 6 hours in S-clone SF-O3 serum-free medium (EIDIA Co., Tokyo, Japan) supplemented with 1% bovine serum albumin (BSA; Sigma, St Louis, MO, USA) with or without 50 ng/mL TPO (Peprotech, Rocky Hill, NJ, USA) at 37°C in a 5% CO_2 atmosphere were used. BM cells were stained with antibodies against cell surface markers, followed, when staining for Bcl-xL and Bcl-2 proteins, by fixation with 0.8% formaldehyde in phosphate-buffered saline and permeabilization with 90% methanol in phosphate-buffered saline. Cells were then incubated with Alexa Fluor 647–conjugated anti–Bcl-xL (Cell Signaling Technology, Danvers, MA, USA) or PE-conjugated anti–Bcl-2 antibody (BD Bioscience, San Jose, CA, USA). Analysis was performed on a FACSAria (BD).

In vitro survival and division of single HSCs

Single-cell cultures of $CD34^{-}$KSL cells were performed under serum-free conditions as described [17,18]. Cells were individually deposited into single wells of a 96-well round-bottom microtiter plate and cultured in S-clone SF-O3 medium supplemented with 1% BSA and 50 ng/mL murine TPO with or without 50 ng/mL murine stem cell factor (SCF; Peprotech). These sorted cells were incubated for 72 hours at 37°C in a 5% CO_2 atmosphere, and then the number of cells in each well was determined under microscopic observation.

Transduction of $CD34^{-}$KSL cells

The retroviral vector GCDNsam (pGCDNsam), with a long terminal repeat derived from murine stem cell virus, has intact splice donor and splice acceptor sequences for generation of subgenomic messenger RNA [19]. Murine *Bcl-xL* cDNA was subcloned into a site upstream of an *IRES-NGFR* construct in pGCDNsam. The shRNAs of control sequence and *Bcl-xL* (SA-Biosciences, Frederick, MD, USA) were subcloned into a site upstream of an *IRES-EGFP* construct in pGCDNsam. To produce recombinant retrovirus, plasmid DNA was transfected into 293gp cells (293 cells containing the *gag* and *pol* genes but lacking an envelope gene) along with a VSV-G expression plasmid by $CaPO_4$ coprecipitation. Supernatants from transfected cells were concentrated by centrifugation at 6000*g* for 16 hours and then resuspended in Dulbecco's modified Eagle's medium (1/300 of the initial volume of the supernatant). 293GPG cells were transduced with the concentrated viral supernatant to establish stable 293GPG cell lines, each capable of producing VSV-G pseudotyped retroviral particles upon Tet-off induction. Infected cells as green fluorescent protein $(GFP)^{+}$ cells were sorted and expanded and then changed to "tetracycline off" medium to produce viral particles. Supernatants were concentrated 300-fold. $CD34^{-}$KSL cells were deposited in 96-well plates at 50 cells per well, and were incubated in α–minimum essential medium supplemented with 1% fetal bovine serum, 100 ng/mL murine SCF, and 100 ng/mL murine TPO for 24 hours. Cells were then transduced with a retrovirus at a multiplicity of infection of 600 in the presence of protamine sulfate (5 μg/mL; Sigma) for 24 hours. After transduction, cells were further incubated in S-clone SF-O3 serum-free medium supplemented with 1% BSA, 50 ng/mL SCF, and 50 ng/mL TPO and subjected to in vitro colony assay or competitive repopulation assay at the indicated time point. In all experiments, transduction efficiency was >80%, as judged from GFP expression observed under an inverted fluorescent microscope.

Colony assays

$CD34^{-}$KSL cells transduced with the indicated retroviruses plated in MethoCult M3434 (Stem Cell Technologies, Vancouver, BC). Culture dishes were incubated at 37°C in a CO_2 atmosphere.

Colony numbers were counted at day 7. Colonies derived from high proliferative potential colony-forming cells were recovered, cytospun onto glass slides, then subjected to May-Grüenwald Giemsa staining for morphological examination.

Competitive repopulation assays

Competitive repopulation assays were performed by using the Ly5 congenic mouse system. In brief, hematopoietic cells from B6-Ly5.1 mice were mixed with BM competitor cells (B6-Ly5.1/5.2) and transplanted into B6-Ly5.2 mice irradiated at a dose of 9.5 Gy. In BM transfer experiment with irradiated HSCs, 50 WT or $Lnk^{-/-}$ CD34$^-$KSL HSCs were sorted into S-clone SF-O3 medium supplemented with 1% BSA, 50 ng/mL SCF, and 50 ng/mL TPO. Sorted cells were irradiated (3.5 Gy) and incubated for 1 hour at 37°C in a CO_2 atmosphere before transfer. In some experiments, 1000 sorted and irradiated (3 Gy or 3.5 Gy) CD34$^-$KSL HSCs were employed. Four and 12 weeks after transplantation, peripheral blood cells of the recipients were stained with PE-conjugated anti-Ly5.1 (A20) or fluorescein isothiocyanate–conjugated anti-Ly5.2 (104) (BioLegend, San Diego, CA, USA). Cells were simultaneously stained with Pacific Blue-conjugated anti-B220 antibody and a mixture of PE-Cy7–conjugated anti-Mac-1 and anti–Gr-1 antibodies or a mixture of allophycocyanin-conjugated anti-CD4 and anti-CD8 antibodies (BioLegend). Cells were analyzed on a FACSAria. The percentage of chimerism was calculated as (percentage donor cells) × 100/(percentage donor cells + percentage recipient cells). When the percentage of chimerism was >1.0 with myeloid, B, and T lymphoid lineages, recipient mice were considered to have been reconstituted by multilineage precursors (positive mice).

Real-time polymerase chain reaction

In the gene expression analysis of HSCs, total RNA was extracted from freshly isolated or incubated CD34$^-$KSL cells using RNeasy Mini Kit (QIAGEN, Valencia, CA, USA), and processed to complementary DNA with Superscript III (Invitrogen, Carlsbad, CA, USA) according to manufacturer's instruction. Polymerase chain reaction (PCR) was done with SYBR Green PCR Master Mix (Perkin-Elmer Applied Biosystem, Foster City, CA, USA) according to manufacturer's instruction. Primer sequences and amplification conditions are available from the authors on request.

Statistical analysis

Mean values of two groups were compared by two-tailed unpaired *t* testing. All statistical analyses were performed on Prism 4 software (GraphPad, San Diego, CA, USA).

Results

Bcl-xL accumulates in Lnk$^{-/-}$ *HSCs in response to TPO*

The absolute number of HSCs in *Lnk*-deficient BM is elevated >16-fold compared with WT BM [9,11]. Nonetheless, in both $Lnk^{-/-}$ and WT, a large proportion of the HSCs in BM is maintained in a quiescent state [11]. We therefore tested the hypothesis that expanded levels of HSCs in $Lnk^{-/-}$ mice might be caused by inhibition of apoptosis through inappropriate activation of antiapoptosis pathways. We first used real-time PCR to analyze gene expression of Bcl-2 family genes (downstream target genes of the JAK-STAT pathway) in WT and in $Lnk^{-/-}$ HSCs with or without TPO signaling. In freshly isolated CD34$^{-/low}$c-Kit$^+$Sca-1$^+$ lineage marker$^-$ (CD34$^-$KSL) cells (the highly enriched HSC fraction in adult murine BM), *Bcl-xL* and *Bcl-2* transcripts were expressed nearly threefold and twofold more in $Lnk^{-/-}$ HSCs than in WT HSCs, respectively (Fig. 1A, B). In WT HSCs, *Bcl-xL* transcripts were downregulated upon stimulation with TPO. In contrast, in $Lnk^{-/-}$ HSCs, expression of the *Bcl-xL* gene was further augmented in response to 6 hours of TPO stimulation (Fig. 1A). Expression of the *Bcl-2* gene was similarly downregulated during TPO stimulation, both in WT and in $Lnk^{-/-}$ HSCs (Fig. 1B). Expression of *Cyclin D1* and *c-Myc*, both of which are also downstream genes of JAK-STAT pathway and critical for cell proliferation, were not significantly affected between WT and $Lnk^{-/-}$ HSCs without TPO stimuli (Supplementary Figure E1A, B; online only, available at www.exphem.org). *Cyclin D1* expression was marginally induced in $Lnk^{-/-}$ HSCs, but not in WT HSCs with TPO stimulation. The expression of *Bax* that is also a member of Bcl-2 family genes and pro-apoptotic gene was upregulated by TPO stimulation, and we did not observe a profound difference between WT and $Lnk^{-/-}$ HSCs (Supplementary Figure E1C; online only, available at www.exphem.org).

We then evaluated the protein levels of Bcl-xL and Bcl-2 in both WT and in $Lnk^{-/-}$ cells, assessing whole BM cells, hematopoietic progenitor cells (c-Kit$^+$ Sca-1$^+$ Lineage$^-$; KSL), and HSCs (CD34$^-$KSL) using intracellular staining and flow cytometric analysis. TPO enhanced expression of Bcl-xL in $Lnk^{-/-}$ KSL cells (mean fluorescence intensity [MFI] = 1955 ± 57) and in CD34$^-$KSL cells (MFI = 1694 ± 45), but not in whole BM cells (MFI = 567 ± 30), or in either WT KSL (MFI = 464 ± 11) or CD34$^-$KSL populations (MFI = 446 ± 23) (Fig. 1C and Supplementary Figure E1D; online only, available at www.exphem.org). These results were similar to those obtained with real-time PCR analysis. No significant difference was detected in the Bcl-2 protein expression levels between WT and $Lnk^{-/-}$ cells regardless of TPO stimuli (Fig. 1D and Supplementary Figure E1D; online only, available at www.exphem.org). Although *Bcl-2* transcripts decreased after TPO stimulation, Bcl-2 protein was slightly elevated in WT as well as in $Lnk^{-/-}$ CD34$^-$KSL cells. The post-translational regulation of Bcl-2 during TPO treatment was not affected by the absence of Lnk/Sh2b3. These data indicate that Lnk/Sh2b3 negatively regulates Bcl-xL expression in a manner dependent upon TPO-c-Mpl signaling.

Radiation resistance of HSCs was increased by the absence of Lnk/Sh2b3

Overexpression of Bcl-2 family genes provides resistance to radiation by its antiapoptotic function [20]. To examine

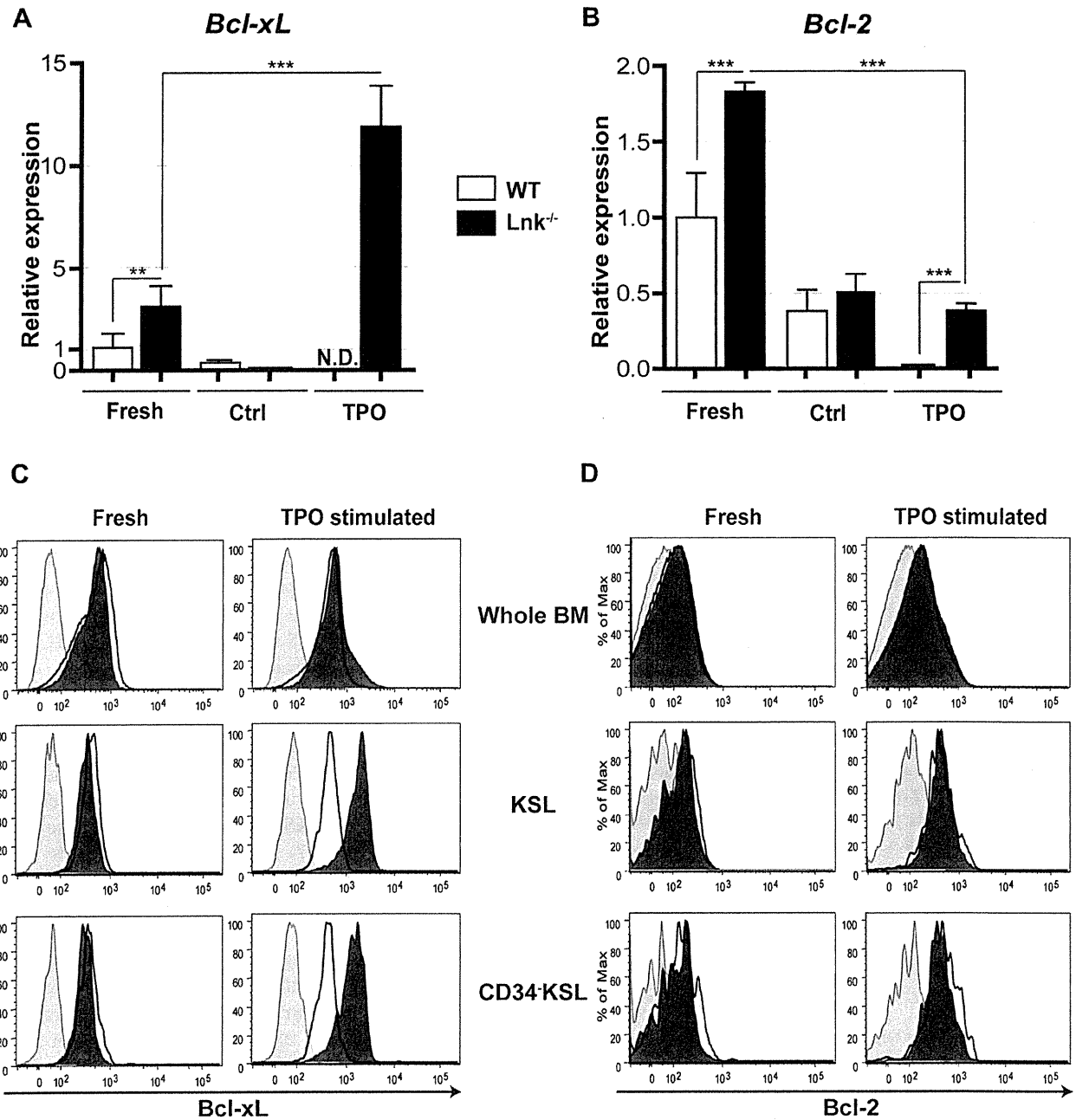

Figure 1. Expression of Bcl-xL and Bcl-2 in WT or $Lnk^{-/-}$ HSCs with or without TPO stimulation. (**A**, **B**) Expression of *Bcl-xL* (**A**), or *Bcl-2* (**B**) messenger RNAs in $CD34^{-}KSL$ cells by quantitative reverse transcription PCR. Fresh: complementary DNA (cDNA) synthesized from freshly isolated $CD34^{-}KSL$ cells. Ctrl: cDNA synthesized from $CD34^{-}KSL$ cells incubated for 6 hours without cytokine stimulation. TPO: cDNA synthesized from $CD34^{-}KSL$ cells incubated for 6 hours in the presence of TPO. Results are shown as mean ± standard deviation of triplicate samples ($^{**}p < 0.01$; $^{***}p < 0.001$). (**C**, **D**) Expression of Bcl-xL (**C**), Bcl-2 (**D**) in BM cells or KSL cells or $CD34^{-}KSL$ cells by flow cytometry. Y axis: cell frequency. X axis: fluorescence intensity as the expression level of Bcl-xL or Bcl-2. Fresh: freshly isolated cells. TPO stimulated: cells incubated for 6 hours in the presence of TPO. Gray-filled histogram: isotype control; blank histogram: WT; black-filled histogram: $Lnk^{-/-}$.

the physiological consequence of marked Bcl-xL upregulation in the absence of Lnk/Sh2b3, we tested whether $Lnk^{-/-}$ HSCs manifested increased resistance to irradiation. As shown in Figure 2A, over several days, both WT and $Lnk^{-/-}$ HSCs proliferated to the same extent without irradiation in the presence of TPO and SCF. After irradiation, although HSCs numbers were reduced by 50% in the first 24 hours, cells started proliferating after 2 or 3 days

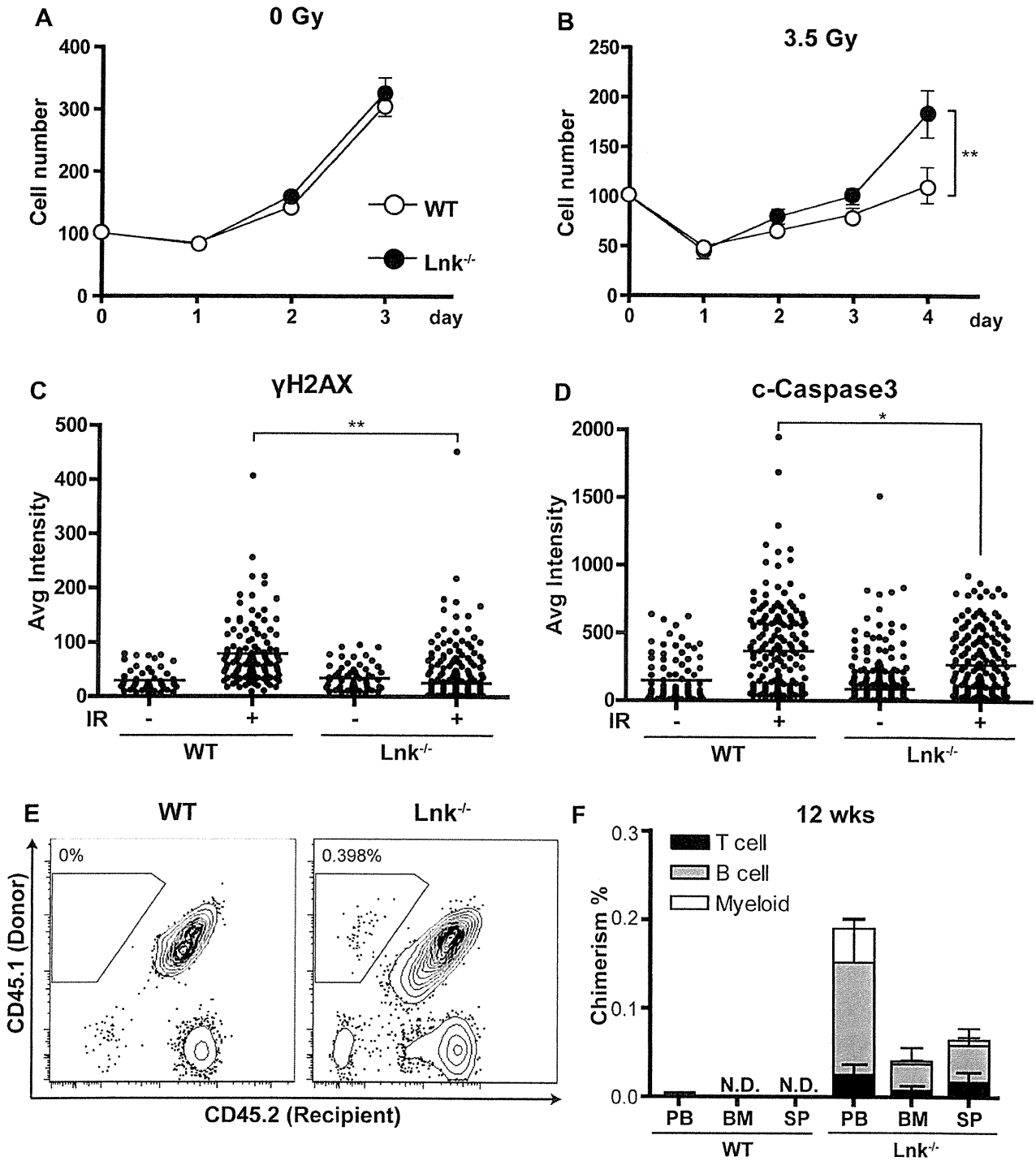

Figure 2. *Lnk*$^{-/-}$ HSCs were resistant to apoptosis by irradiation. (**A**, **B**) Growth of WT or *Lnk*$^{-/-}$ CD34^{-}KSL HSCs after irradiation. One hundred freshly isolated CD34^{-}KSL cells were exposed to x-rays [0 Gy (**A**) or 3.5 Gy (**B**)] and cultured in the presence of SCF and TPO for 3 to 4 days (**$p < 0.01$). (**C**, **D**) Immunostaining of γH2AX (**C**) and c-caspase 3 (**D**) in CD34^{-}KSL HSCs with or without irradiation (3.5 Gy). Results are shown as average intensities of fluorescence-conjugated secondary antibodies analyzed by ArrayScan VTI HCS reader (*$p < 0.05$, **$p < 0.01$). (**E**, **F**) Fifty irradiated (3.5 Gy) WT or *Lnk*$^{-/-}$ CD34^{-}KSL HSCs (Ly5.1) were transferred into lethally irradiated recipient mice (Ly5.2) with 5×10^5 competitor WT BM cells (Ly5.1/5.2). (**E**) Flow cytometric analysis of a recipient mouse 12 weeks after BM transfer. (**F**) Chimerism of donor-derived cells in the peripheral blood, BM, and spleen (SP) of recipient mice 12 weeks post-BM transfer. Results are shown as mean ± standard deviation with n = 5.

(Fig. 2B and Supplementary Figure E2A, B; online only, available at www.exphem.org). Under the same conditions, the increasing rate of $Lnk^{-/-}$ HSC numbers was significantly higher than WT HSCs (Fig. 2B and Supplementary Figure E2A, B; online only, available at www.exphem.org). Although WT and $Lnk^{-/-}$ HSCs died after receiving a radiation dose of >5 Gy, the $Lnk^{-/-}$ HSCs survived longer periods than WT cells (data not shown). To clarify whether the phenotype observed with the $Lnk^{-/-}$ HSCs was due to resistance to irradiation by a reduction in apoptosis or superior recovery by increased cell division postirradiation, we compared survival and cell division rates between WT and $Lnk^{-/-}$ HSCs with or without irradiation. By stimulation with TPO, the frequency of cell division in $Lnk^{-/-}$ HSCs was greater than that in WT HSCs at 72 hours of incubation (Supplementary Figure E2D; online only, available at www.exphem.org) as we reported previously [12]. After irradiation, cell division was almost abolished, however, surviving cells were more frequently observed in $Lnk^{-/-}$ HSCs compared to WT HSCs (Supplementary Figure E2C, D, and E; online only, available at www.exphem.org). In the presence of SCF and TPO, we also found that the frequency of surviving cells without division was significantly increased in $Lnk^{-/-}$ HSCs, although the enforced cell division was almost comparable to WT HSCs. These results indicated that $Lnk^{-/-}$ HSCs were more resistant to irradiation by a reduction in apoptosis.

We next used immunostaining to investigate the expression level of γH2AX, which recognizes DNA double-strand breaks, and the level of cleaved (c)-caspase 3, an activated form of caspase 3 that acts as a lethal protease at the most distal stage of apoptosis in irradiated HSCs. The fluorescence intensities of both γH2AX and c-caspase 3 were increased in WT HSCs after exposure to radiation (Fig. 2C, D). Induction levels of those proteins were significantly milder or slower in $Lnk^{-/-}$ HSCs compared to WT HSCs (Fig. 2C, D). To further demonstrate their functional resistance to radiation, we transferred irradiated HSCs from WT or $Lnk^{-/-}$ mice into lethally irradiated recipient mice with competitor BM cells and determined their reconstitutional ability. As expected, none of the mice were reconstituted with WT HSC-derived cells treated with 3.5 Gy of radiation (Fig. 2E, F). The reconstitution ability of $Lnk^{-/-}$ HSCs is originally superior to WT (Supplementary Figure E2F; online only, available at www.exphem.org). However, even when 10^3 WT HSCs irradiated with 3 Gy were transplanted, there was no indication of engraftment (Supplementary Figure E2G; online only, available at www.exphem.org). In the case of $Lnk^{-/-}$ HSCs, the same radiation dose (3.5 Gy) did not eliminate reconstitutional ability (Supplementary Figure E2H; online only, available at www.exphem.org). Long-term engraftment of irradiated HSCs, as well as their differentiation to multilineage cells, was observed in recipient mice (Fig. 2E, F). $Lnk^{-/-}$ HSC-derived blood cells were detected in the peripheral blood, spleen, and BM of recipient mice 12 weeks post-transfer (Fig. 2F). These results demonstrated that $Lnk^{-/-}$ HSCs had increased protective capacity against apoptosis induced by irradiation due to enhanced expression of Bcl-xL.

Downregulation of Bcl-xL normalized the repopulating ability of $Lnk^{-/-}$ *HSCs*

To investigate whether enhanced accumulation of Bcl-xL in HSCs promoted their self-renewal and reconstitutional abilities, we constructed retrovirally mediated overexpression and knockdown systems for *Bcl-xL*. We confirmed protein expression of Bcl-xL HeLa cells retrovirally transduced with a Bcl-xL-expressing vector, but not in nontransduced or mock-transduced HeLa cells (Supplementary Figure E3A; online only, available at www.exphem.org). We also verified downregulation of *Bcl-xL* by transduction of *Bcl-xL* shRNA into HeLa cells expressing *Bcl-xL* (Supplementary Figure E3B; online only, available at www.exphem.org). Using this knockdown vector, we evaluated the effects of Bcl-xL reduction in early multilineage progenitors using colony assays and by analyzing the frequency of colony-forming unit granulocyte/erythroblast/macrophage/megakaryocyte. In the presence of cytokines supporting differentiation into all hematopoietic lineages, we downregulated the level of Bcl-xL in WT and in $Lnk^{-/-}$ $CD34^-KSL$ cells and observed a slight reduction of total colony numbers and frequency of colony-forming unit granulocyte/erythroblast/macrophage/megakaryocyte mixed colonies in colony-forming assay compared with control shRNA-transduced cells (Fig. 3A). These data suggest that the expression level of Bcl-xL in HSCs might not be critical for short-term repopulating ability of HSCs. We sought to determine the effect of reduced Bcl-xL expression in $Lnk^{-/-}$ HSCs on long-term repopulation ability in vivo, by performing competitive repopulation assays. Fifty sorted $CD34^-KSL$ cells were transduced with vectors and cultured for 5 days ex vivo and transferred to recipient mouse with competitor BM cells. The multilineage repopulation capacity of *Bcl-xL* shRNA-transduced $Lnk^{-/-}$ HSCs was decreased compared with control shRNA-transduced HSCs and returned to a level comparable to that of WT HSCs (Fig. 3B and Supplementary Figure E3C; online only, available at www.exphem.org). Analysis of donor-derived cells in each hematopoietic lineage revealed that the augmented capacity of $Lnk^{-/-}$ HSCs to repopulate the B-cell compartment was normalized almost to the level nearly comparable that of WT HSCs following downregulation of *Bcl-xL* (Fig. 3C and Supplementary Figure E3D; online only, available at www.exphem.org). We further examined BM transfer of control or *Bcl-xL*-shRNA transduced WT HSCs into recipient mice with competitor BM cells. The repopulation ability of *Bcl-xL*-shRNA transduced WT HSCs was almost comparable to control vector transduced HSCs (Fig. 3D),

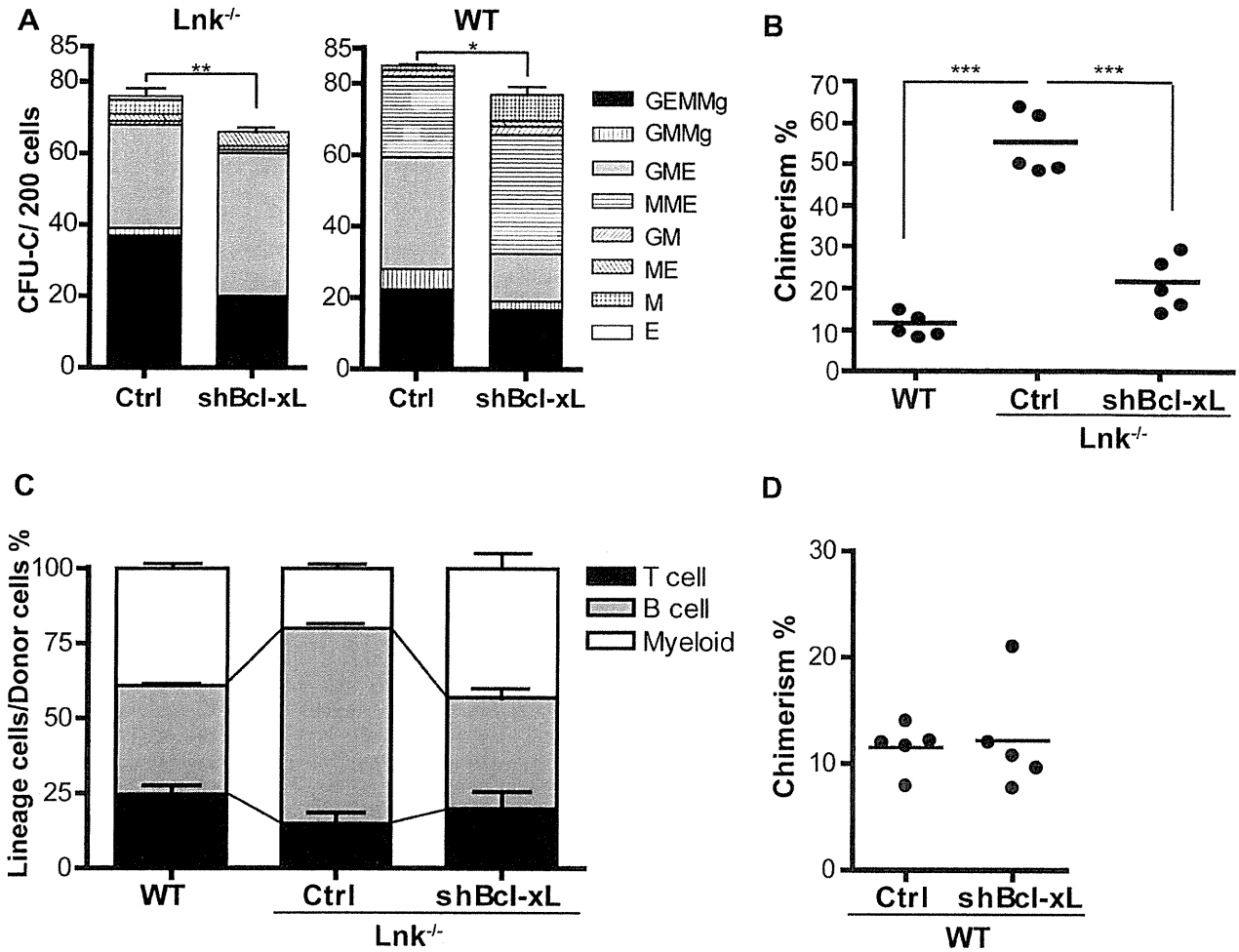

Figure 3. Loss of function of *Bcl-xL* from $Lnk^{-/-}$ HSCs inhibits their repopulation activity in vivo. (**A**) In vitro colony assay of HSCs with downregulated Bcl-xL. $Lnk^{-/-}$ (left) or WT (right) $CD34^{-}KSL$ cells were transduced with control sequence (Ctrl) or shRNA-*Bcl-xL* (shBcl-xL) and plated in methylcellulose medium to allow colony formation 36 hours after initiation of transduction. GFP^{+} colonies, which were derived from colony-forming cells (CFCs), were counted at day 7 and recovered for morphological analysis to evaluate the frequency of colony types. Results are shown as mean ± standard deviation of triplicate experiments ($*p < 0.05$; $**p < 0.01$). (**B, C**) Fifty $CD34^{-}KSL$ cells from Ly5.1 $Lnk^{-/-}$ mice were transduced with either Ctrl or shBcl-xL. Five days after transduction, cells were injected into lethally irradiated Ly5.2 recipient mice along with Ly5.1/5.2 competitor cells. (**B**) Chimerism of Ctrl or shBcl-xL transduced $Lnk^{-/-}$ HSC-derived cells in peripheral blood (PB) of recipient mice 12 weeks post-BM transplantation. Results are shown as mean ± standard deviation, n = 5 ($***p < 0.001$). WT represents transplantation of 50 WT $CD34^{-}KSL$ cells without transduction as control. (**C**) The percentages of individual lineages/GFP^{+} $CD45.1^{+}$ donor-derived cells in PB of recipient mice (n = 5) 12 weeks post-transplantation. T cells are $CD4^{+}$ or $CD8^{+}$ cells. B cells are $B220^{+}$ cells. Myeloid cells are Gr-1^{+} or Mac-1^{+} cells. (**D**) Fifty $CD34^{-}KSL$ cells from Ly5.1 WT mice were transduced with either Ctrl or shBcl-xL. Five days after transduction, cells were injected into lethally irradiated Ly5.2 recipient mice along with Ly5.1/5.2 competitor BM cells. Chimerism of Ctrl or shBcl-xL transduced WT HSC-derived $CD45^{+}$ cells in PB of recipient mice 12 weeks post-BM transplantation.

indicating that Bcl-xL silencing by itself did not affect HSC functions independently of the Lnk-mediated regulation. These data indicated that Bcl-xL accumulation was one of the critical events to enhance the repopulating ability of HSCs by protecting them from apoptosis, and that the Bcl-xL expression was regulated by Lnk/Sh2b3 in HSCs.

Discussion

We previously demonstrated that Lnk/Sh2b3 negatively regulates self-renewal of HSCs by modifying TPO-mediated signal transduction [12]. We also showed that significant enhancement of STAT5 activation led to increased long-term repopulating activity of $Lnk^{-/-}$ HSCs. In this study, we identified the key molecule that functions downstream of the JAK2-STAT5 signaling pathway and regulates the survival and repopulating activity of HSCs in $Lnk^{-/-}$ mice. Expression of Bcl-xL and Bcl-2 was significantly upregulated in $Lnk^{-/-}$ HSCs compared to normal HSCs. Bcl-xL was further upregulated in $Lnk^{-/-}$ HSCs upon stimulation with TPO, but not in normal cells. Bcl-xL reportedly inhibits apoptosis when cells undergo DNA damage [21]. Consistent

with their high expression of Bcl-xL, *Lnk*$^{-/-}$ HSCs retained their proliferative activity and repopulation capacity even after exposure to radiation that abrogated growth and engraftment of WT HSCs. The induction of γH2AX was decreased or delayed in irradiated *Lnk*$^{-/-}$ HSCs compared with WT HSCs. Experiments showed that the accumulation of Bcl-xL or Bcl-2 leads to cell cycle arrest at G_0 because of the diminished activity of cyclins D/cdk4 and E/cdk2 in conjunction with increased levels of p27 [22]. Thus, our data suggest that irradiated *Lnk*$^{-/-}$ HSCs showed a delayed DNA damage response because of their overexpression of Bcl-xL. Furthermore, the decrease in c-caspase 3 activity in irradiated *Lnk*$^{-/-}$ HSCs indicated that upregulation of Bcl-xL provided enhanced protection against apoptosis.

Cells overexpressing Bcl-xL or Bcl-2 present very similar phenotypes, i.e., resistance to apoptosis and cell cycle arrest. BM precursors in *Bcl-xL* and *Bcl-2* transgenic mice show increased reconstitution ability due to their anti-apoptotic functions [23,24]. *Bcl-xL*–deficient mice die around embryonic day 13 due to extensive apoptosis of hematopoietic cells [25], although *Bcl-2*–deficient mice remain viable [26], suggesting that Bcl-xL has more critical functions in hematopoiesis than Bcl-2, although partially redundant. We examined whether enhanced repopulating ability of HSCs in the absence of Lnk/Sh2b3 was due to their increased expression of Bcl-xL. Downregulation of *Bcl-xL* by shRNA in *Lnk*$^{-/-}$ HSCs resulted in a significant reduction of repopulation ability compared to WT HSCs. These results suggest that Bcl-xL is a key molecule with critical functions for hematopoiesis, functions that are regulated in an Lnk/Sh2b3-dependent manner.

Recently, disease-related *LNK/SH2B3* mutations were reported in patients with JAK2 V617F-negative myeloproliferative neoplasms that exhibited aberrant JAK-STAT activation [27]. Antiapoptotic Bcl-2 and Bcl-xL were highly expressed in patients with myelodysplastic syndrome or acute myeloid leukemia compared with proapoptotic Bax/Bad [28]. Considering these findings together with our own observation, HSCs in patients carrying a mutation in either the *LNK/SH2B3* or *JAK2* gene, or carrying a *Bcr-Abl* translocation could become resistant to apoptosis due to enhanced expression of Bcl-xL mediated by activation of TPO signaling, which would facilitate accumulation of HSCs or progenitors. Furthermore, the antiapoptotic effects of Bcl-xL can facilitate accumulation of oncogenic mutations, leading to development of myeloproliferative disorders. Gery et al. demonstrated that overexpression of *Lnk/Sh2b3* in Ba/F3 cells transduced with a myeloproliferative leukemia oncogene mutant inhibited cytokine-independent growth by blocking activation of JAK2, STAT3, Erk, and Akt [29]. In our present study, knockdown of *Bcl-xL* in *Lnk*$^{-/-}$ HSCs significantly decreased their repopulating capacity as well as WT HSCs. These findings might suggest that regulation of Lnk/Sh2b3 in combination with Bcl-xL will provide new insights into the pathogenesis of myeloproliferative disorders and could help in the development of new therapeutic approaches.

Acknowledgments

We thank Y. Ishii for excellent technical assistance, Dr. M. Onodera and Mr. Y. Ichida for providing 293GPG cells transduced with *Bcl-xL*.

This work was supported in part by grants from the Ministry of Education, Culture, Sport, Science and Technology, Japan.

Author contributions: N.S. and S.Y. designed and performed experiments and analyzed data. S.T. contributed *Lnk*$^{-/-}$ mice. N.S., S.Y., and S.T. wrote the manuscript. H.N., H.E., and T.Y. provided advice on the manuscript.

Conflict of interest disclosure

No financial interest/relationship with financial interest relating to the topic of this article has been declared.

References

1. Calvi LM, Adams GB, Weibrecht KW, et al. Osteoblastic cells regulate the haematopoietic stem cell niche. Nature. 2003;425:841–846.
2. Li W, Johnson SA, Shelley WC, Yoder MC. Hematopoietic stem cell repopulating ability can be maintained in vitro by some primary endothelial cells. Exp Hematol. 2004;32:1226–1237.
3. Mendez-Ferrer S, Michurina TV, Ferraro F, et al. Mesenchymal and haematopoietic stem cells form a unique bone marrow niche. Nature. 2010;466:829–834.
4. Omatsu Y, Sugiyama T, Kohara H, et al. The essential functions of adipo-osteogenic progenitors as the hematopoietic stem and progenitor cell niche. Immunity. 2010;33:387–399.
5. Sauvageau G, Thorsteinsdottir U, Eaves CJ, et al. Overexpression of HOXB4 in hematopoietic cells causes the selective expansion of more primitive populations in vitro and in vivo. Genes Dev. 1995;9:1753–1765.
6. Antonchuk J, Sauvageau G, Humphries RK. HOXB4 overexpression mediates very rapid stem cell regeneration and competitive hematopoietic repopulation. Exp Hematol. 2001;29:1125–1134.
7. Takaki S, Morita H, Tezuka Y, Takatsu K. Enhanced hematopoiesis by hematopoietic progenitor cells lacking intracellular adaptor protein, Lnk. J Exp Med. 2002;195:151–160.
8. Takaki S, Watts JD, Forbush KA, et al. Characterization of Lnk. An adaptor protein expressed in lymphocytes. J Biol Chem. 1997;272:14562–14570.
9. Ema H, Sudo K, Seita J, et al. Quantification of self-renewal capacity in single hematopoietic stem cells from normal and Lnk-deficient mice. Dev Cell. 2005;8:907–914.
10. Tong W, Lodish HF. Lnk inhibits Tpo-mpl signaling and Tpo-mediated megakaryocytopoiesis. J Exp Med. 2004;200:569–580.
11. Bersenev A, Wu C, Balcerek J, Tong W. Lnk controls mouse hematopoietic stem cell self-renewal and quiescence through direct interactions with JAK2. J Clin Invest. 2008;118:2832–2844.
12. Seita J, Ema H, Ooehara J, et al. Lnk negatively regulates self-renewal of hematopoietic stem cells by modifying thrombopoietin-mediated signal transduction. Proc Natl Acad Sci U S A. 2007;104:2349–2354.
13. Socolovsky M, Fallon AE, Wang S, Brugnara C, Lodish HF. Fetal anemia and apoptosis of red cell progenitors in Stat5a-/-5b-/- mice: a direct role for Stat5 in Bcl-X(L) induction. Cell. 1999;98:181–191.
14. Socolovsky M, Nam H, Fleming MD, et al. Ineffective erythropoiesis in Stat5a(-/-)5b(-/-) mice due to decreased survival of early erythroblasts. Blood. 2001;98:3261–3273.

15. Osawa M, Hanada K, Hamada H, Nakauchi H. Long-term lymphohematopoietic reconstitution by a single CD34-low/negative hematopoietic stem cell. Science. 1996;273:242–245.
16. Sudo K, Ema H, Morita Y, Nakauchi H. Age-associated characteristics of murine hematopoietic stem cells. J Exp Med. 2000;192:1273–1280.
17. Takano H, Ema H, Sudo K, Nakauchi H. Asymmetric division and lineage commitment at the level of hematopoietic stem cells: inference from differentiation in daughter cell and granddaughter cell pairs. J Exp Med. 2004;199:295–302.
18. Iwama A, Oguro H, Negishi M, et al. Enhanced self-renewal of hematopoietic stem cells mediated by the polycomb gene product Bmi-1. Immunity. 2004;21:843–851.
19. Kaneko S, Onodera M, Fujiki Y, Nagasawa T, Nakauchi H. Simplified retroviral vector gcsap with murine stem cell virus long terminal repeat allows high and continued expression of enhanced green fluorescent protein by human hematopoietic progenitors engrafted in non-obese diabetic/severe combined immunodeficient mice. Hum Gene Ther. 2001;12:35–44.
20. Domen J, Gandy KL, Weissman IL. Systemic overexpression of BCL-2 in the hematopoietic system protects transgenic mice from the consequences of lethal irradiation. Blood. 1998;91:2272–2282.
21. Boise LH, Gonzalez-Garcia M, Postema CE, et al. bcl-x, a bcl-2-related gene that functions as a dominant regulator of apoptotic cell death. Cell. 1993;74:597–608.
22. Janumyan YM, Sansam CG, Chattopadhyay A, et al. Bcl-xL/Bcl-2 coordinately regulates apoptosis, cell cycle arrest and cell cycle entry. EMBO J. 2003;22:5459–5470.
23. Mata M, Chiffoleau E, Adler SH, et al. Bcl-XL expression in stem cells facilitates engraftment and reduces the need for host conditioning during bone marrow transplantation. Am J Transplant. 2004;4:58–64.
24. Domen J, Cheshier SH, Weissman IL. The role of apoptosis in the regulation of hematopoietic stem cells: overexpression of Bcl-2 increases both their number and repopulation potential. J Exp Med. 2000;191:253–264.
25. Motoyama N, Wang F, Roth KA, et al. Massive cell death of immature hematopoietic cells and neurons in Bcl-x-deficient mice. Science. 1995;267:1506–1510.
26. Veis DJ, Sorenson CM, Shutter JR, Korsmeyer SJ. Bcl-2-deficient mice demonstrate fulminant lymphoid apoptosis, polycystic kidneys, and hypopigmented hair. Cell. 1993;75:229–240.
27. Oh ST, Simonds EF, Jones C, et al. Novel mutations in the inhibitory adaptor protein LNK drive JAK-STAT signaling in patients with myeloproliferative neoplasms. Blood. 2010;116:988–992.
28. Parker JE, Mufti GJ, Rasool F, et al. The role of apoptosis, proliferation, and the Bcl-2-related proteins in the myelodysplastic syndromes and acute myeloid leukemia secondary to MDS. Blood. 2000;96:3932–3938.
29. Gery S, Gueller S, Nowak V, et al. Expression of the adaptor protein Lnk in leukemia cells. Exp Hematol. 2009;37:585–592.e2.